



Accuracies of field CO₂–H₂O data from open-path eddy-covariance flux systems: Assessment based on atmospheric physics and biological environment

Xinhua Zhou^{1,2}, Tian Gao^{1,3}, Ning Zheng^{1,4}, Yanlei Li^{1,2}, Fengyuan Yu^{1,3}, Tala Awada⁵, Jiaojun Zhu^{1,3}

- 5 ¹ Ker Research and Development, CAS Key Laboratory of Forest Ecology and Management, Institute of Applied Ecology, Chinese Academy of Sciences, Shenyang 110015, China
² Campbell Scientific Inc., Logan, UT 84321, USA
³ Qingyuan Forest CERN, National Observation and Research Station, Liaoning Province, Shenyang 110015, China
⁴ Beijing Servirst Technology Limited, Beijing 102299, China
10 ⁵ School of Natural Resources, University of Nebraska, Lincoln, NE 68583, USA

Correspondence to: Tian Gao (tiangao@iae.ac.cn) and Ning Zheng (ning.zheng@servirst.com)

Abstract. Ecosystem CO₂–H₂O data measured vastly from open-path eddy-covariance (OPEC) systems by infrared analyzers have numerous applications in biogeosciences. To assess the applicability, data uncertainties from measurements
15 are needed. The uncertainties are sourced from infrared analyzers in zero drift, gain drift, cross-sensitivity, and precision variability. The sourced uncertainties are individually specified for analyzer performance, but no methodology exists to comprehend these individual uncertainties into a cumulative error for the specification of an overall accuracy, which is ultimately needed. Using the methodology for close-path eddy-covariance systems, this accuracy for OPEC systems is determined from all individual uncertainties via an accuracy model further formulated into CO₂ and H₂O accuracy equations.
20 Based on atmospheric physics and the biological environment, these equations are used to evaluate CO₂ accuracy (± 1.21 mgCO₂ m⁻³, relatively $\pm 0.19\%$) and H₂O accuracy (± 0.10 gH₂O m⁻³, relatively $\pm 0.18\%$ in saturated air at 35 °C and 101.325 kPa). Cross-sensitivity and precision variability are minor, although unavoidable, uncertainties. Zero drifts and gain drifts are major uncertainties but are adjustable via corresponding zero and span procedures during field maintenance. The equations provide rationales to assess and guide the procedures. In an atmospheric CO₂ background, CO₂ zero and span procedures can
25 narrow CO₂ accuracy by 40%, from ± 1.21 to ± 0.72 mgCO₂ m⁻³. In hot and humid weather, H₂O gain drift potentially adds more to H₂O measurement uncertainty, which requires more attention. If H₂O zero and span procedures can be performed practically from 5 to 35 °C, the poorest H₂O accuracy can be improved by 30%, from ± 0.10 to ± 0.07 gH₂O m⁻³. Under freezing conditions, an H₂O span is both impractical and unnecessary, but the zero procedure becomes imperative to minimize H₂O measurement uncertainty. In cold/dry conditions, the zero procedure for H₂O, along with CO₂, is an
30 operational and efficient option to ensure and improve H₂O accuracy.



1 Introduction

Open-path eddy-covariance (OPEC) systems are used most to measure boundary-layer CO₂, H₂O, heat, and momentum fluxes between ecosystems and the atmosphere (Lee and Massman, 2011). For the fluxes, an OPEC system is equipped with a fast-response three-dimensional (3-D) sonic anemometer, to measure 3-D wind and sonic temperature (T_s), and a fast-response infrared CO₂-H₂O analyzer (hereafter referred to as an infrared analyzer or analyzer) to measure CO₂ and H₂O fluctuations (Fig. 1). In this system, the analyzer is adjacent to the sonic measurement volume. Both anemometer and analyzer together provide high-frequency (e.g., 10 to 20 Hz) measurements, which are used to compute the fluxes at a location represented by the measurement volume (Aubinet et al., 2012). The degree of exactness for each flux from computations depends on the field measurement exactness of variables such as CO₂, H₂O, T_s , and 3-D wind (Foken et al., 2012). Beyond flux computations, the data for individual variables from these field measurements are important in numerous applications. Knowledge of measurement exactness is required for data analysis and applicability assessment (Csavina et al., 2017; Hill et al., 2017).

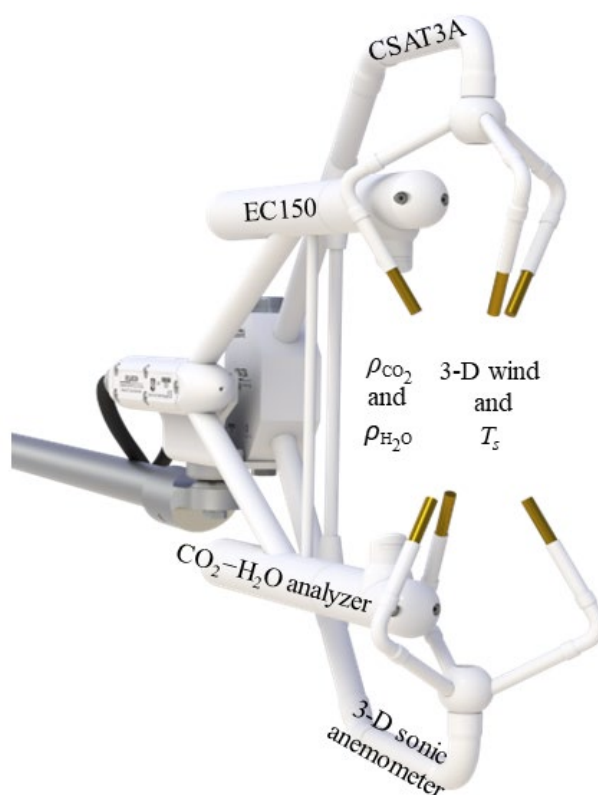


Figure 1. Integration of a CSAT3A sonic anemometer for three-dimensional (3-D) wind and sonic temperature (T_s) and an EC150 infrared CO₂-H₂O analyzer for CO₂ density (ρ_{CO_2}) and H₂O density ($\rho_{\text{H}_2\text{O}}$) in an open-path eddy-covariance flux system (Campbell Scientific Inc., UT, USA).



The infrared analyzers in OPEC systems output CO₂ density (ρ_{CO_2} in mgCO₂ m⁻³) and H₂O density (ρ_{H_2O} in gH₂O m⁻³). For instance, ρ_{H_2O} , along with T_s and atmospheric pressure (P), can be used to derive ambient air temperature (T_a) (Swiatek, 2018). In this case, given an exact equation of T_a in terms of the three independent variables ρ_{H_2O} , T_s , and P , the applicability of the equation to the OPEC systems for T_a depends wholly on the measurement exactness of the three independent variables. The higher the degree of exactness, the less uncertain T_a . The assessment on the applicability needs the measurement exactness.

Although the CO₂ and H₂O data uncertainty sources, such as analyzer zero and gain drifts, analyzer background sensitivities, and measurement precision variability, are separately specified (LI-COR Biosciences, 2021b; Campbell Scientific Inc., 2021b), the specification for overall exactness of an individual field CO₂ or H₂O measurement is unavailable due to the absence of methodology to composite all of the specified measurement uncertainties into a cumulative error. For any sensor, the measurement exactness depends on its performances as commonly specified in terms of accuracy, precision, and other uncertainty descriptors such as sensor drift. Conventionally, accuracy is defined as a systematic uncertainty, and precision is defined as a random measurement error (ISO, 2012, where ISO is the acronym of International Organization for Standardization). Other uncertainty descriptors are also defined for specific reliability in measurement performance. For example, CO₂ zero drift is one of the descriptors specified for the performance of infrared analyzers in CO₂ measurements (Campbell Scientific Inc., 2021b). Both accuracy and precision are universally applicable to any sensor for the specification of its performance in measurement exactness. Other uncertainty descriptors are more sensor-specific (e.g., cross-sensitivity to CO₂/H₂O is used for infrared analyzers in OPEC systems).

Conventionally, sensor accuracy is the degree of closeness to which its measurements are to the true value in the measured variable; sensor precision, related to repeatability, is the degree to which repeated measurements under unchanged conditions show the same values (Joint Committee for Guides in Metrology, 2008). Another definition advanced by the ISO (2012), revising the conventional definition of accuracy as trueness originally representing only systematic uncertainty, specifies accuracy as the combination of both trueness and precision. An advantage of this definition of accuracy is that it consolidates all measurement uncertainties. According to this definition, the accuracy is the range of cumulative uncertainty from all sources in field measurements. For close-path eddy-covariance (CPEC) systems, Zhou et al. (2021) developed a method and derived a model for the assessment on this accuracy of CO₂/H₂O measurements by infrared analyzers. Their model was further formulated as equations to evaluate the defined accuracies of CO₂ and H₂O data from CPEC systems. Although the CPEC systems are very different from OPEC systems in measurement designs (e.g., Measurements take place inside a closed cuvette vs. in an open space) and in computation variables (e.g., CO₂/H₂O mixing ratio vs. CO₂/H₂O density), there are similarities between CPEC and OPEC systems in measurement uncertainties as specified by their manufacturers (Campbell Scientific Inc., 2021a; 2021b) because the infrared analyzers in both systems use the same physics theories and similar optical techniques for their measurement (LI-COR Biosciences, 2021a; 2021b). Accordingly, the method developed by Zhou et al. (2021) for CPEC systems should be reasonably applicable to their OPEC counterparts although the model



80 needs rederivation and equations needs reformulation. Following the methodology of Zhou et al. (2021) and using the
 specifications of EC150 infrared analyzers in OPEC systems as an example (Campbell Scientific Inc., 2021b), we derive the
 model and formulate equations to assess the accuracies of CO₂ and H₂O measurements from OPEC systems by infrared
 analyzers, discuss the uses of accuracies in data applications and analyzer field maintenance, and ultimately provide an
 reference for the flux measurement community to specify the overall accuracy of field CO₂/H₂O measurements from OPEC
 85 systems by infrared analyzers.

2 Specification implications

An OPEC system for this study includes, but is not limited to, a CSAT3A sonic anemometer for a fast response to 3-D wind
 and T_s , and an EC150 infrared analyzer for a fast response to CO₂ and H₂O (Fig. 1). The system operates in a T_a range from
 –30 to 50 °C and in a P range from 70 to 106 kPa. Within both ranges, the specifications for CO₂ and H₂O measurements
 90 (Campbell Scientific Inc., 2021b) are given in Table 1.

Table 1. Measurement specifications for EC150 infrared CO₂–H₂O analyzers

	CO ₂			H ₂ O			Note
	notation	value	unit	notation	value	unit	
Calibration range		0 – 1,553	mgCO ₂ m ⁻³		0 – 44	gH ₂ O m ⁻³	For CO ₂ up to 4,500 mgCO ₂ m ⁻³ if specially needed. Zero/gain drift is the possible maximum range within the system operational ranges in ambient air temperature (T_a) and atmospheric pressure. The actual drift depends more on T_a .
Zero drift	d_{cz}	±0.55	mgCO ₂ m ⁻³	d_{wz}	±0.04	gH ₂ O m ⁻³	
Gain drift	d_{cg}	±0.10% ^{a/} true ρ_{CO_2}	mgCO ₂ m ⁻³	d_{wg}	±0.30% ^{b/} true ρ_{H_2O}	gH ₂ O m ⁻³	
Cross-sensitivity to H ₂ O	s_{H_2O}	±2.69×10 ⁻⁷	mgCO ₂ m ⁻³ (gH ₂ O m ⁻³) ⁻¹		N/A		
Cross-sensitivity to CO ₂		N/A		s_{CO_2}	±4.09×10 ⁻⁵	gH ₂ O m ⁻³ (mgCO ₂ m ⁻³) ⁻¹	
Precision	σ_{CO_2}	0.200	mgCO ₂ m ⁻³	σ_{H_2O}	0.004	gH ₂ O m ⁻³	

^a 0.10% is the CO₂ gain drift percentage denoted by $\delta_{CO_2_g}$ in text, and ρ_{CO_2} is CO₂ density.

^b 0.30% is the H₂O gain drift percentage denoted by $\delta_{H_2O_g}$ in text, and ρ_{H_2O} is H₂O density.

95 In Table 1, the top limit of 1,553 mgCO₂ m⁻³ in the calibration range for CO₂ density in dry air is more than double
 the atmospheric background CO₂ density of 760 mgCO₂ m⁻³, equal to 415 $\mu\text{molCO}_2 \text{ mol}^{-1}$, where mol is for a dry air unit,



reported by Global Monitoring Laboratory (2021) with a T_a of 20 °C under a P of 101.325 kPa (i.e., normal temperature and pressure - Wright et al. (2003)). The top limit of 44 gH₂O m⁻³ in the calibration range for H₂O density is equivalent to a 37 °C dew point, higher than the highest 35 °C dew point ever recorded under natural conditions on the Earth (National Weather Service, 2021).

The measurement uncertainties of infrared analyzers for CO₂ and H₂O in Table 1 are specified by individual uncertainty components along with their magnitudes: zero drift, gain drift, cross-sensitivity to CO₂/H₂O, and precision variability. Zero drift uncertainty is an analyzer non-zero response to zero air/gas (i.e., air/gas free of CO₂ and H₂O). Gain drift uncertainty is an analyzer trend-deviation response to measured gas species away from its true value in proportion (Campbell Scientific Inc., 2021b). Cross-sensitivity is an analyzer background response to either CO₂ if H₂O is measured, or H₂O if CO₂ is measured. Precision variability is an analyzer random response to minor unexpected factors. For CO₂ and H₂O, respectively, these four components should be composited as a cumulative uncertainty to evaluate the accuracy that is ultimately needed in applications.

Precision variability is a random error, and the other specifications can be considered as trueness. Zero drifts are impacted more by T_a , and so are gain drifts. Additionally, each gain drift is also positively proportional to the true magnitude of CO₂/H₂O density (i.e., true ρ_{CO_2} or true ρ_{H_2O}) under measurements. Lastly, cross-sensitivity to H₂O/CO₂ is related to the background amount of H₂O/CO₂ as indicated by its units, mgCO₂ m⁻³ (gH₂O m⁻³)⁻¹ for CO₂ measurements, and gH₂O m⁻³ (mgCO₂ m⁻³)⁻¹ for H₂O measurements.

Accordingly, beyond statistical analysis, the accuracy of CO₂/H₂O measurements should be evaluated over a T_a range of -30 to 50 °C, a ρ_{H_2O} range of up to 44 gH₂O m⁻³, and a ρ_{CO_2} range of up to 1,553 mgCO₂ m⁻³.

3 Accuracy model

The measurement accuracy of infrared analyzers is the maximum range of cumulative measurement uncertainty from the four components uncertainties as specified in Table 1: zero drift, gain drift, cross-sensitivity, and precision variability. The four uncertainties interactionally or independently add uncertainties to a measurement value. Given the true α density ($\rho_{\alpha T}$, where subscript α can be either CO₂ or H₂O) and measured α density (ρ_α), the difference between the true and measured α densities ($\Delta\rho_\alpha$) is given by

$$\Delta\rho_\alpha = \rho_\alpha - \rho_{\alpha T}. \quad (1)$$

The analyzer overestimates the true value if $\Delta\rho_\alpha > 0$, exactly estimates the true value if $\Delta\rho_\alpha = 0$, and underestimates the true value if $\Delta\rho_\alpha < 0$. The measurement accuracy is the maximum range of overestimation or underestimation, being a range of $\Delta\rho_\alpha$ (i.e., an accuracy range). According to the analyses of Zhou et al. (2021) for CPEC infrared analyzers, this range is interactionally contributed by the zero drift uncertainty ($\Delta\rho_\alpha^z$), gain drift uncertainty ($\Delta\rho_\alpha^g$), and cross-sensitivity uncertainty ($\Delta\rho_\alpha^s$) while being independently added by the precision uncertainty ($\Delta\rho_\alpha^p$). However, any interactional



130 contribution from a pair of uncertainties is three orders smaller in magnitude than each in the pair. The contribution of interactions to the accuracy range can be reasonably neglected. Therefore, the accuracy range can be modeled as a simple sum of the four components uncertainties. From Eq. (A7) in Appendix A, the measurement accuracy of α density from OPEC systems by infrared analyzers is defined in an accuracy model as

$$\Delta\rho_{\alpha} \equiv \pm\left(\left|\Delta\rho_{\alpha}^z\right| + \left|\Delta\rho_{\alpha}^g\right| + \left|\Delta\rho_{\alpha}^s\right| + \left|\Delta\rho_{\alpha}^p\right|\right). \quad (2)$$

Assessment on the accuracy of field CO₂ or H₂O measurements is to formulate and evaluate the four terms on the right side of this accuracy model.

135 4 Accuracy of CO₂ density measurements

Accuracy Model (2) defines the accuracy of field CO₂ measurements from OPEC systems by infrared analyzers ($\Delta\rho_{CO_2}$) as

$$\Delta\rho_{CO_2} \equiv \pm\left(\left|\Delta\rho_{CO_2}^z\right| + \left|\Delta\rho_{CO_2}^g\right| + \left|\Delta\rho_{CO_2}^s\right| + \left|\Delta\rho_{CO_2}^p\right|\right), \quad (3)$$

where $\Delta\rho_{CO_2}^z$ is CO₂ zero drift uncertainty, $\Delta\rho_{CO_2}^g$ is CO₂ gain drift uncertainty, $\Delta\rho_{CO_2}^s$ is cross-sensitivity-to-H₂O uncertainty, and $\Delta\rho_{CO_2}^p$ is CO₂ precision uncertainty.

140 CO₂ precision is the standard deviation of ρ_{CO_2} random errors among repeated measurements under the same conditions (Joint Committee for Guides in Metrology, 2008). Therefore, using this deviation, the precision uncertainty for an individual CO₂ measurement at a 95% confidence interval (P-value of 0.05) can be statistically formulated as (Hoel, 1984)

$$\Delta\rho_{CO_2}^p = \pm 1.96 \times \sigma_{CO_2}. \quad (4)$$

145 The other uncertainties, due to CO₂ zero drift, CO₂ gain drift, and cross-sensitivity-to-H₂O, are caused by the inability of the working equation inside an infrared analyzer to be adapted to the changes in its internal and ambient environmental conditions, such as internal housing CO₂ and/or H₂O levels and ambient air temperature. According to LI-COR Biosciences (2021b), a general model of the working equation for ρ_{CO_2} is given by

$$\rho_{CO_2} = P \sum_{i=1}^5 a_{ci} \left\{ 1 - \left[\frac{A_c}{A_{cs}} + S_w \left(1 - \frac{A_w}{A_{ws}} \right) \right] Z_c \right\}^i \left\{ \frac{G_c}{P} \right\}^i, \quad (5)$$

150 where subscripts c and w indicate CO₂ and H₂O, respectively; a_{ci} ($i = 1, 2, 3, 4,$ or 5) is a coefficient of the five-order polynomial in the terms inside curly brackets; A_{cs} and A_{ws} are the power values of analyzer source lights in the wavelengths for CO₂ and H₂O measurements, respectively; A_c and A_w are their respective remaining power values after the source lights pass through the measured air; S_w is cross-sensitivity of the detector to H₂O, while detecting CO₂, in the wavelength for CO₂ measurements (hereafter referred to as sensitivity-to-H₂O); Z_c is the CO₂ zero adjustment (i.e., CO₂ zero coefficient); and G_c is the CO₂ gain adjustment (i.e., commonly known as the CO₂ span coefficient). For an individual analyzer, the parameters a_{ci} , Z_c , G_c , and S_w in Model (5) are statistically estimated in the production calibration against a series of standard CO₂ gases



at different concentration levels over the ranges of ρ_{H_2O} and P (hereafter referred to as calibration). The estimated parameters are specific for the analyzer; therefore, Model (5) with these estimated parameters becomes an analyzer-specific CO_2 working equation. The working equation is used inside the infrared analyzer to compute ρ_{CO_2} from field measurements of A_c , A_{cs} , A_w , A_{ws} , and P .

160 The analyzer-specific working equation is deemed accurate immediately after calibration (LI-COR Biosciences, 2021b). However, as used inside an optical instrument under changing environments vastly different from its manufacturing conditions, the working equation may not be fully adaptable to the changes, which might be reflected through CO_2 zero and/or gain drifts of the infrared analyzers in measurements. In the working equation for ρ_{CO_2} from Model (5), the parameter Z_c is related to CO_2 zero; G_c , to CO_2 gain; and S_w , to sensitivity-to- H_2O . Therefore, the analyses of Z_c and G_c , along with S_w ,
165 are an approach to understand the causes of CO_2 zero drift, CO_2 gain drift, and sensitivity-to- H_2O . Such understanding is necessary to formulate $\Delta\rho_{CO_2}^z$, $\Delta\rho_{CO_2}^g$, and $\Delta\rho_{CO_2}^s$ in Model (3).

4.1 Z_c and $\Delta\rho_{CO_2}^z$ (CO_2 zero drift uncertainty)

An infrared analyzer was calibrated for zero air/gas to report zero ρ_{CO_2} plus an unavoidable random error. However, during use of the analyzer in measurement environments that are different from calibration conditions, the analyzer often gradually
170 reports this zero ρ_{CO_2} value that is different from zero and possibly beyond $\pm\Delta\rho_{CO_2}^p$, which is known as CO_2 zero drift. This drift is primarily affected by the temperature surrounding the analyzer away from the calibration temperature and/or by traceable CO_2 and H_2O accumulations during use inside the analyzer light housing due to an inevitable, although extremely little, leaking exchange of housing air with ambient air (hereafter referred to as housing CO_2 - H_2O accumulation). The light housing is technically sealed to keep housing air close to zero air by implementing scrubber chemicals into the housing to
175 absorb any CO_2 and H_2O that may sneak into the housing through an exchange with any ambient air (LI-COR Biosciences, 2021b).

Due to the CO_2 zero drift, the working equation needs to be adjusted through its parameter re-estimation to adapt the ambient air temperature and housing CO_2 - H_2O accumulation near which the system is running. This adjustment technique is the zero procedure, which brings the ρ_{CO_2} and ρ_{H_2O} of zero air/gas from the working equation back to zero as closely as
180 possible. In this section, ignoring ρ_{H_2O} , the discussion focus will be on CO_2 , although applicability to H_2O also exists. In the field, the zero procedure must be simple. The simplest way is to use one air/gas benchmark to re-estimate one parameter in the working equation. This parameter must be adjustable to output zero ρ_{CO_2} from the zero air/gas benchmark. It is Z_c indeed (see Model (5)), being adjustable to result in a zero ρ_{CO_2} value for zero air/gas, if re-estimated for the working equation from Model (5) by



$$185 \quad Z_c = \left[\frac{A_{c0}}{A_{cs}} + S_w \left(1 - \frac{A_{w0}}{A_{ws}} \right) \right]^{-1}, \quad (6)$$

where A_{c0} and A_{w0} are the counterparts of A_c and A_w for zero air/gas, respectively. Inside an analyzer, the zero procedure for CO_2 is to re-estimate Z_c to balance Eq. (6).

If Z_c could continually balance Eq. (6) after the zero procedure, the CO_2 zero drift would not be significant; however, this is not the case. Similar to its performance after calibration, an analyzer may still drift after the zero procedures due to changing ambient air temperature and/or CO_2 - H_2O accumulation. Nevertheless, the value of Z_c , which should be used with the ambient air temperature surrounding the infrared analyzer and particularly with housing CO_2 - H_2O accumulation, is unpredictable. Assuming that the scrubber chemicals inside the analyzer light housing is replaced as per the recommended maintenance schedule, the housing CO_2 - H_2O accumulation should not be a concern while the air temperature surrounding the infrared analyzer is not controlled. Therefore, the CO_2 zero drift of analyzers is specified to be influenced more by T_a and to be $\pm 0.55 \text{ mgCO}_2 \text{ m}^{-3}$ as its maximum range within the operational ranges in T_a and P of OPEC systems (Table 1). This specification is the maximum range of CO_2 measurement uncertainty due to the CO_2 zero drift.

Given that an analyzer performs best, even without zero drift, at the ambient air temperature for the calibration/zeroing procedure (T_c), and that it possibly drifts while T_a gradually changes away from T_c , then the further away T_a is from T_c , the more it possibly drifts. Over the operational range in P of OPEC systems, this drift is more proportional to the difference between T_a and T_c but is still within the specifications (Campbell Scientific Inc., 2021b). Accordingly, CO_2 zero drift uncertainty at T_a can be formulated as

$$200 \quad \Delta \rho_{\text{CO}_2}^z = \frac{d_{cz}}{T_{rh} - T_{rl}} \times \begin{cases} T_a - T_c & T_c < T_a < T_{rh} \\ T_c - T_a & T_c > T_a > T_{rl} \end{cases}, \quad (7)$$

where, over the operational range in T_a of OPEC systems, T_{rh} is the highest-end value ($50 \text{ }^\circ\text{C}$) and T_{rl} is the lowest-end value ($-30 \text{ }^\circ\text{C}$, Table 1). $\Delta \rho_{\text{CO}_2}^z$ from this equation has the maximum range, as specified in Table 1, equal to d_{cz} in magnitude as if T_a and T_c were separately at the two ends of operational range in T_a of OPEC systems.

4.2 G_c and $\Delta \rho_{\text{CO}_2}^g$ (CO_2 gain drift uncertainty)

An infrared analyzer was also calibrated against a series of standard CO_2 gases. The calibration sets the working equation from Model (5) to closely follow the gain trend of change in ρ_{CO_2} . As was determined with the zero drift, the analyzer, with changes in internal CO_2 - H_2O accumulation and ambient measurement conditions during use, could report CO_2 gradually away from the real gain trend of the change in ρ_{CO_2} , which is specifically termed CO_2 gain drift. This drift is affected by almost the same factors as the CO_2 zero drift (LI-COR Biosciences, 2021b).



Due to the gain drift, the infrared analyzer needs to be further adjusted, after the zero procedure, to tune its working equation back to the real gain trend in ρ_{CO_2} of measured air as close as possible. This is done with the CO₂ span procedure. Like the zero procedure, this procedure is simplified by the use of one CO₂ span gas, as a benchmark, with a known CO₂ amount ($\tilde{\rho}_{CO_2}$) around the typical CO₂ density values in the measurement environment. Also, because one CO₂ value from CO₂ span gas is used, only one parameter in the working equation is available for adjustment. Weighing the gain of the working equation more than any other parameter, this parameter is the CO₂ span coefficient (G_c) (see Model (5)). The CO₂ span is used to re-estimate G_c to satisfy the following equation (for details, see LI-COR Biosciences, 2021b)

$$\left| \tilde{\rho}_{CO_2} - \rho_{CO_2}(G_c) \right| \leq \min \left| \tilde{\rho}_{CO_2} - \rho_{CO_2} \right|. \quad (8)$$

Similar to the zero drift, the CO₂ gain drift continues after the CO₂ span procedure. Based on a similar consideration for the specifications of CO₂ zero drift, the CO₂ gain drift is specified by the maximum CO₂ gain drift percentage ($\delta_{CO_2-g} = 0.1\%$) associated with ρ_{CO_2} as $\pm 0.10\% \times (\text{true } \rho_{CO_2})$ (Table 1). This specification is the maximum range of CO₂ measurement uncertainty due to the CO₂ gain drift within the operational ranges in T_a and P of OPEC systems.

Given that an analyzer performs best, almost without gain drift, at the ambient air temperature for calibration/span procedure (also denoted by T_c , because zero and span procedures should be performed under similar ambient air temperature conditions) but also drifts while T_a gradually changes away from T_c , then the further away T_a is from T_c , the greater potential the drift has. Accordingly, the same approach to the formulation of CO₂ zero drift uncertainty can be applied to the formulation of approximate equation for CO₂ gain drift uncertainty at T_a as

$$\Delta \rho_{CO_2}^g \equiv \pm \frac{\delta_{CO_2-g} \rho_{CO_2 T}}{T_{rh} - T_{rl}} \times \begin{cases} T_a - T_c & T_c < T_a < T_{rh} \\ T_c - T_a & T_c > T_a > T_{rl} \end{cases}, \quad (9)$$

where $\rho_{CO_2 T}$ is true CO₂ density unknown in measurement. Given that the measured value of CO₂ density is represented by ρ_{CO_2} , by referencing Eq. (1), $\rho_{CO_2 T}$ can be expressed as

$$\rho_{CO_2 T} = \rho_{CO_2} - (\Delta \rho_{CO_2}^z + \Delta \rho_{CO_2}^g + \Delta \rho_{CO_2}^s + \Delta \rho_{CO_2}^p). \quad (10)$$

The term inside the parentheses in this equation is the measurement error for $\rho_{CO_2 T}$ that is reasonably smaller in magnitude, by at least two orders, than $\rho_{CO_2 T}$, whose magnitude in atmospheric background under the normal temperature and pressure as used by Wright et al. (2003) is 760 mgCO₂ m⁻³ (Global Monitoring Laboratory, 2021). Therefore, ρ_{CO_2} in Eq. (10) is the best alternative, with the most likelihood, to $\rho_{CO_2 T}$ for the application of Eq. (9). As such, $\rho_{CO_2 T}$ in Eq. (9) can be reasonably approximated by ρ_{CO_2} for equation applications. Using this approximation, Eq. (9) becomes

$$\Delta \rho_{CO_2}^g = \pm \frac{\delta_{CO_2-g} \rho_{CO_2}}{T_{rh} - T_{rl}} \times \begin{cases} T_a - T_c & T_c < T_a < T_{rh} \\ T_c - T_a & T_c > T_a > T_{rl} \end{cases}. \quad (11)$$

With measured ρ_{CO_2} , this equation is applicable in estimating the CO₂ gain drift uncertainty. The gain drift uncertainty



240 $(\Delta\rho_{CO_2}^s)$ from this equation has the maximum range of $\pm\delta_{CO_2_g} \rho_{CO_2}$, as if T_a and T_c were separately at the two ends of operational range in T_a of OPEC systems. With the most likelihood, this maximum range is the closest to $\pm\delta_{CO_2_g} \times (\text{true } \rho_{CO_2})$ as specified in Table 1.

4.3 S_w and $\Delta\rho_{CO_2}^s$ (sensitivity-to-H₂O uncertainty)

The infrared wavelength of 4.3 μm for CO₂ measurements is minorly absorbed by H₂O (LI-COR Biosciences, 2021b; 245 Campbell Scientific Inc., 2021b). This minor absorption slightly interferes with the absorption by CO₂ in the wavelength (McDermitt et al., 1993). The power of the same measurement light through several gas samples with the same CO₂ density, but different backgrounds of H₂O densities, is detected with different values of A_c for the working equation from Model (5). Without parameter S_w and its joined term in the working equation, different A_c values must result in significantly different ρ_{CO_2} values, although they are actually the same. To report the same ρ_{CO_2} for air flows with the same CO₂ density under 250 different H₂O backgrounds, the different values of A_c to report similar ρ_{CO_2} are accounted for by S_w associated with A_w and A_{ws} in the working equation from Model (5). Similar to Z_c and G_c in the equation, S_w is not perfectly accurate and can have uncertainty in the determination of ρ_{CO_2} . This uncertainty for EC150 infrared analyzers is specified by sensitivity-to-H₂O (s_{H_2O}) as $\pm 2.69 \times 10^{-7} \text{ mgCO}_2 \text{ m}^{-3} (\text{gH}_2\text{O m}^{-3})^{-1}$ (Table 1). As indicated by its unit, this uncertainty is linearly related to ρ_{H_2O} . Assuming the analyzer for CO₂ works best, without this uncertainty, in dry air, $\Delta\rho_{CO_2}^s$ could be formulated as

$$255 \quad \Delta\rho_{CO_2}^s \equiv s_{H_2O} \rho_{H_2O} \quad 0 \leq \rho_{H_2O} \leq 44 \text{ gH}_2\text{O m}^{-3}. \quad (12)$$

Accordingly, $\Delta\rho_{CO_2}^s$ can be in a range of

$$\Delta\rho_{CO_2}^s \leq 44 |s_{H_2O}|. \quad (13)$$

4.4 $\Delta\rho_{CO_2}$ (CO₂ measurement accuracy)

Substituting Eqs. (4), (7), (11), and (13) into Model (3), $\Delta\rho_{CO_2}$ for an individual CO₂ measurement can be expressed as

$$260 \quad \Delta\rho_{CO_2} = \pm \left[1.96\sigma_{CO_2} + 44 |s_{H_2O}| + \frac{|d_{cz}| + \delta_{CO_2_g} \rho_{CO_2}}{T_{rh} - T_{rl}} \times \begin{cases} T_a - T_c & T_c < T_a < T_{rh} \\ T_c - T_a & T_c > T_a > T_{rl} \end{cases} \right]. \quad (14)$$

This is the CO₂ accuracy equation for the OPEC systems with infrared analyzers. It expresses the accuracy of a field CO₂ measurement from the OPEC systems in terms of its specifications σ_{CO_2} , s_{H_2O} , d_{cz} , $\delta_{CO_2_g}$, and the OPEC system operational range in T_a as indicated by T_{rh} and T_{rl} ; measured variables ρ_{CO_2} and T_a ; and a known variable T_c . Given the specifications and the known variable, this equation can be used to evaluate the CO₂ accuracy as a range in relation to T_a and ρ_{CO_2} .



265 4.5 Evaluation of $\Delta\rho_{CO_2}$

Given the analyzer specifications, the accuracy of field CO_2 measurements from an infrared analyzer after calibration, zero, and/or span at T_c can be evaluated using the CO_2 accuracy equation (14) over a domain of T_a and ρ_{CO_2} . To visualize the relationship of accuracy with T_a and ρ_{CO_2} , the accuracy is presented better as the ordinate along the abscissa of T_a for ρ_{CO_2} at different levels and must be evaluated within possible maximum ranges of T_a and ρ_{CO_2} in ecosystems. In evaluation, the T_a is limited to the -30 to 50 °C range within which OPEC systems operate, T_c can be assumed to be 20 °C (i.e., standard air temperature as used by Wright et al. (2003)), and ρ_{CO_2} can be ranged according to its variation in ecosystems.

4.5.1 ρ_{CO_2} range

CO_2 density measured by the infrared analyzers ranges up to $1,553$ $mgCO_2$ m^{-3} . In the atmosphere, its CO_2 background mixing ratio currently is 415 $\mu molCO_2$ mol^{-1} (Global Monitoring Laboratory, 2021). Under the normal temperature and pressure conditions (Wright et al., 2003), this background mixing ratio is equivalent to 760 $mgCO_2$ m^{-3} in dry air. CO_2 density in ecosystems commonly ranges from 650 to $1,500$ $mgCO_2$ m^{-3} (LI-COR Biosciences, 2021b), depending on biological processes (Wang et al., 2016), aerodynamic regimes (Yang et al., 2007), and thermodynamic states (Ohkubo et al., 2008). In this study, this range is extended from 600 to $1,600$ $mgCO_2$ m^{-3} as a common range within which $\Delta\rho_{CO_2}$ is evaluated. Because of the dependence of $\Delta\rho_{CO_2}$ on ρ_{CO_2} (Eq. 14), to show the accuracy at different CO_2 levels, the range is further divided into five grades of 600 , 760 (atmospheric background), 1000 , 1300 , and 1600 $mgCO_2$ m^{-3} for evaluation presentations as in Fig. 2.

According to the brief review by Zhou et al. (2021) on the plant physiological threshold in air temperature for growth and development and the soil temperature dynamic related to CO_2 from microorganism respiration and/or wildlife activities in terrestrial ecosystems, ρ_{CO_2} at any grade of $1,000$, 1300 , or 1600 $mgCO_2$ m^{-3} should start, at 5 °C, to converge asymptotically to the atmospheric CO_2 background (760 $mgCO_2$ m^{-3} at -30 °C, Fig. 2). Without the asymptotical function for the convergence curve, conservatively assuming the convergence has a simple linear trend with T_a from 5 to -30 °C, $\Delta\rho_{CO_2}$ is evaluated up to the magnitude of ρ_{CO_2} along the trend (Fig. 2).

4.5.2 $\Delta\rho_{CO_2}$ range

At $T_a = T_c$, the CO_2 accuracy is best at its narrowest range as the sum of precision and and sensitivity-to- H_2O uncertainties (± 0.39 $mgCO_2$ m^{-3}). However, away from T_c , its range near-linearly becomes wider. The $\Delta\rho_{CO_2}$ range can be summarized as $\pm 0.40 - \pm 1.21$ $mgCO_2$ m^{-3} over the domain of T_a and ρ_{CO_2} (Fig. 2a and CO_2 columns in Table 2). The maximum CO_2 relative accuracy at the different levels of ρ_{CO_2} is in a range of $\pm 0.07\%$ at $1,600$ $mgCO_2$ m^{-3} to 0.19% at 600 $mgCO_2$ m^{-3} (from data for Fig. 2b).

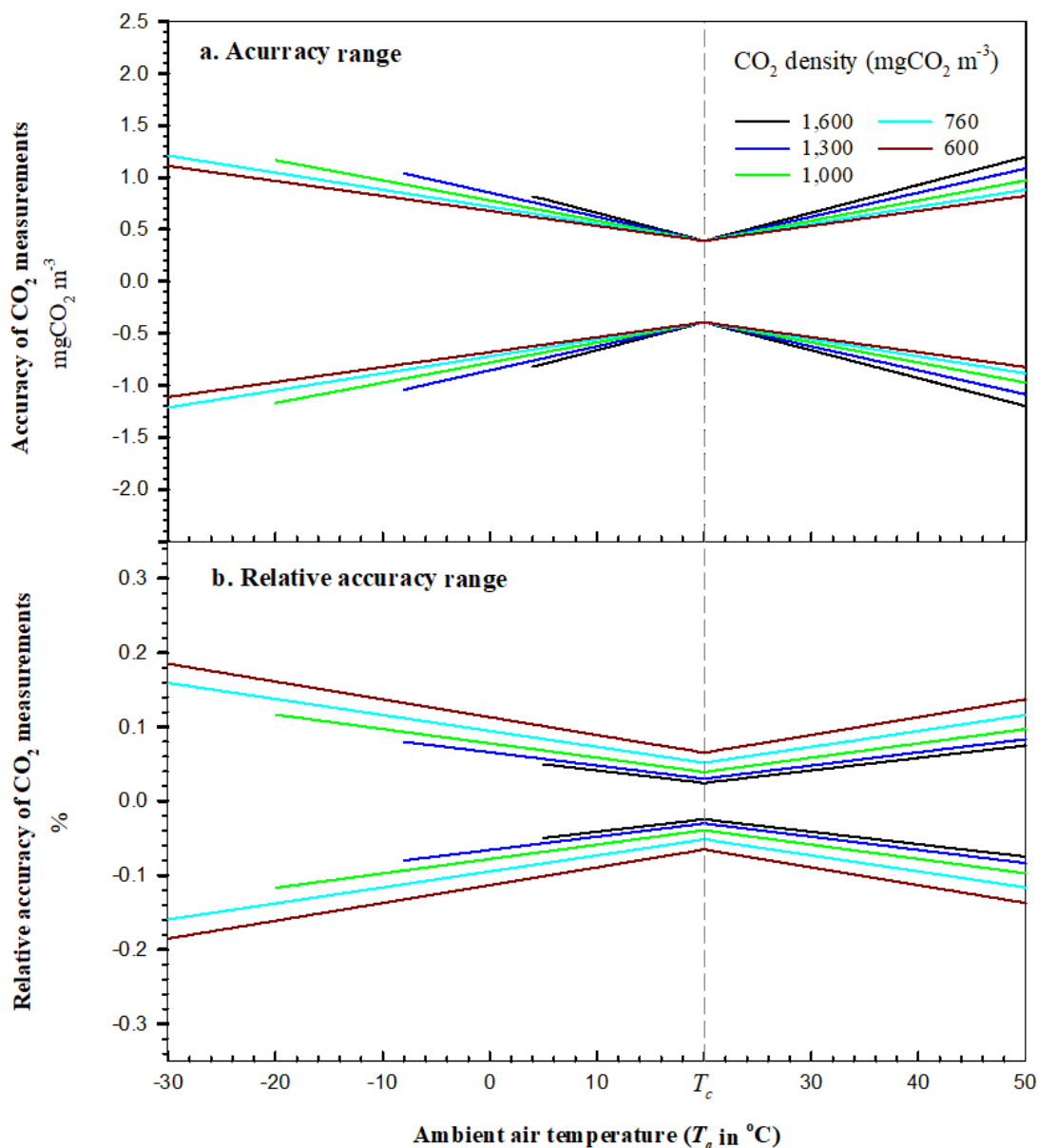


Figure 2. Accuracy of field CO₂ measurements from open-path eddy-covariance flux systems by EC150 infrared CO₂-H₂O analyzers over their operational range in T_a at atmospheric pressure of 101.325 kPa. The vertical dashed line represents ambient temperature T_c at which an analyzer was calibrated, zeroed, and/or spanned. Above 5 °C, accuracy is evaluated up to the possible maximum CO₂ density in ecosystems (black curve). Assume this maximum starts linearly decreasing at 5 °C to the atmospheric CO₂ background (760 mgCO₂ m⁻³) at -30 °C. Accordingly, below 5 °C, the accuracy for CO₂ density at a level above the background (green, blue, or black curve) is evaluated up to this decreasing trend. Relative accuracy of CO₂ measurements is the ratio of CO₂ accuracy to CO₂ density.



305

Table 2. Accuracies of field CO₂ and H₂O measurements from open-path eddy-covariance systems by EC150 infrared CO₂–H₂O analyzers on the major values of background ambient air temperature, CO₂, and H₂O in ecosystems. (Atmospheric pressure: 101.325 kPa. Calibration ambient air temperature: 20 °C.)

Ambient air temperature °C	CO ₂				H ₂ O			
	760 mgCO ₂ m ⁻³ a/		1,600 mgCO ₂ m ⁻³ b/		60% Relative humidity		Saturated	
	Accuracy ± mgCO ₂ m ⁻³	Relative accuracy ± %	Accuracy ± mgCO ₂ m ⁻³	Relative accuracy ± %	Accuracy ± gH ₂ O m ⁻³	Relative accuracy ± %	Accuracy ± gH ₂ O m ⁻³	Relative accuracy ± %
-30	1.211	0.16			0.066	32.14	0.066	19.36
-25	1.129	0.15			0.063	19.01	0.064	11.47
-22	1.080	0.14			0.062	14.00	0.062	8.46
-20	1.047	0.14			0.061	11.46	0.062	6.94
-18	1.014	0.13			0.060	9.41	0.061	5.70
-15	0.965	0.13			0.059	7.04	0.060	4.28
-12	0.916	0.12		N/A ^{c/}	0.058	5.30	0.058	3.23
-10	0.883	0.12			0.057	4.40	0.058	2.68
-7	0.834	0.11			0.055	3.34	0.057	2.05
-5	0.801	0.11			0.055	2.79	0.056	1.71
-2	0.752	0.10			0.053	2.14	0.055	1.32
0	0.720	0.09			0.052	1.80	0.054	1.11
2	0.687	0.09			0.052	1.54	0.053	0.95
5	0.638	0.08	0.795	0.05	0.050	1.22	0.052	0.76
7	0.605	0.08	0.741	0.05	0.049	1.05	0.051	0.65
10	0.556	0.07	0.661	0.04	0.047	0.84	0.049	0.52
13	0.507	0.07	0.580	0.04	0.046	0.67	0.047	0.41
15	0.474	0.06	0.526	0.03	0.044	0.57	0.045	0.35
18	0.425	0.06	0.446	0.03	0.042	0.45	0.042	0.28
20	0.392	0.05	0.392	0.02	0.040	0.39	0.040	0.23
22	0.425	0.06	0.446	0.03	0.042	0.36	0.043	0.22
25	0.474	0.06	0.526	0.03	0.045	0.33	0.047	0.20
28	0.523	0.07	0.607	0.04	0.049	0.30	0.052	0.19
30	0.556	0.07	0.661	0.04	0.052	0.29	0.057	0.19
32	0.589	0.08	0.715	0.04	0.055	0.27	0.062	0.18
35	0.638	0.08	0.795	0.05	0.061	0.26	0.070	0.18
37	0.670	0.09	0.849	0.05	0.066	0.25	0.077	0.17
40	0.720	0.09	0.930	0.06	0.073	0.24		
45	0.801	0.11	1.064	0.07	0.090	0.23		
48	0.851	0.11	1.145	0.07	0.099	0.23		N/A ^{d/}
50	0.883	0.12	1.198	0.07		N/A ^{c/}		

^a 760 mgCO₂ m⁻³ is the atmospheric background CO₂ density.

^b 1,600 mgCO₂ m⁻³ is assumed to be the maximum CO₂ density in ecosystems.



^c CO₂ density in ecosystems is assumed to be lower than 1,600 mgCO₂ m⁻³ when ambient air temperatures is below 5 °C.

^d H₂O density in saturated air above 37 °C is out of the measurement range of EC150 infrared CO₂-H₂O analyzers (0 – 44 gH₂O m⁻³).

^e H₂O density in air of 60% relative humidity above 48 °C is out of the measurement range of EC150 infrared CO₂-H₂O analyzers (0 – 44 gH₂O m⁻³).

5 Accuracy of H₂O density measurements

Model (2) defines the accuracy of field H₂O measurements from OPEC systems by infrared analyzers ($\Delta\rho_{H_2O}$) as

$$\Delta\rho_{H_2O} \equiv \pm \left(\left| \Delta\rho_{H_2O}^z \right| + \left| \Delta\rho_{H_2O}^g \right| + \left| \Delta\rho_{H_2O}^s \right| + \left| \Delta\rho_{H_2O}^p \right| \right), \quad (15)$$

where $\Delta\rho_{H_2O}^z$ is H₂O zero drift uncertainty, $\Delta\rho_{H_2O}^g$ is H₂O gain drift uncertainty, $\Delta\rho_{H_2O}^s$ is cross-sensitivity-to-CO₂ uncertainty, and $\Delta\rho_{H_2O}^p$ is H₂O precision uncertainty. Using the same approach for $\Delta\rho_{CO_2}^p$, $\Delta\rho_{H_2O}^p$ is formulated as

$$\Delta\rho_{H_2O}^p = \pm 1.96 \times \sigma_{H_2O}. \quad (16)$$

The other uncertainty terms in Model (15) can be understood and formulated using the similar approach for their counterparts in Model (3).

5.1 $\Delta\rho_{H_2O}^z$ (H₂O zero drift uncertainty) and $\Delta\rho_{H_2O}^g$ (H₂O gain drift uncertainty)

The model of the analyzer working equation for ρ_{H_2O} is similar to Model (5) for ρ_{CO_2} in formulation, given by (LI-COR Biosciences, 2021b)

$$\rho_{H_2O} = P \sum_{i=1}^3 a_{wi} \left\{ 1 - \left[\frac{A_w}{A_{ws}} + S_c \left(1 - \frac{A_c}{A_{cs}} \right) \right] Z_w \right\}^i \left\{ \frac{G_w}{P} \right\}^i, \quad (17)$$

where a_{wi} ($i = 1, 2, \text{ or } 3$) is a coefficient of the three-order polynomial in the terms inside curly brackets; S_c is the cross-sensitivity of a detector to CO₂, while detecting H₂O, in the wavelength for H₂O measurements (hereafter referred to as sensitivity-to-CO₂); Z_w is the H₂O zero adjustment (i.e., H₂O zero coefficient); and G_w is the H₂O gain adjustment (i.e., commonly referred as to H₂O span coefficient). The parameters of a_{wi} , Z_w , G_w , and S_c in Model (17) are statistically estimated to establish an H₂O working equation in production calibration against a series of air standards with different H₂O contents under ranges of ρ_{CO_2} and P (i.e., calibration). The H₂O working equation (i.e., Model 17 with estimated parameters) is used inside the analyzer to compute ρ_{H_2O} from field measurements of A_w , A_{ws} , A_c , A_{cs} , and P .

Because of the similarity in model principles and parameter implications between Models (5) and (17), using the same analyses and rationales as for $\Delta\rho_{CO_2}^z$ and $\Delta\rho_{CO_2}^g$, $\Delta\rho_{H_2O}^z$ is formulated as



$$\Delta\rho_{H_2O}^z = \frac{d_{wz}}{T_{rh} - T_{rl}} \times \begin{cases} T_a - T_c & T_c < T_a < T_{rh} \\ T_c - T_a & T_c > T_a > T_{rl} \end{cases}, \quad (18)$$

335 and $\Delta\rho_{H_2O}^g$ is formulated as

$$\Delta\rho_{H_2O}^g = \pm \frac{\delta_{H_2O_g}\rho_{H_2O}}{T_{rh} - T_{rl}} \times \begin{cases} T_a - T_c & T_c < T_a < T_{rh} \\ T_c - T_a & T_c > T_a > T_{rl} \end{cases}. \quad (19)$$

5.2 $\Delta\rho_{H_2O}^s$ (sensitivity-to-CO₂ uncertainty)

The infrared light at wavelength of 2.7 μm for H₂O measurement is traceably absorbed by CO₂ (see Fig. 4.7 in Wallace and Hobbs, 2006). This absorption interferes slightly with the absorption by H₂O in the wavelength (McDermitt et al., 1993). As
 340 such, the power of identical measurement lights through several air standards with the same H₂O density but different backgrounds of CO₂ amounts would result in different values of A_w into the H₂O working equation from Model (17). In this equation, without parameter S_c and its joined term, different A_w values will result in significantly different ρ_{H_2O} values, although ρ_{H_2O} is essentially the same. To report the same ρ_{H_2O} for air flows with the same H₂O amount under different CO₂ backgrounds, different values of A_w to report the same ρ_{H_2O} are accounted for by S_c associated with A_c and A_{cs} in the H₂O
 345 working equation (see Model 17). However, S_c is not perfectly accurate, either, having uncertainty in the determination of ρ_{H_2O} . This uncertainty in the EC150 infrared analyzer is specified by the sensitivity-to-CO₂ (s_{CO_2}) value as the maximum range of $\pm 4.09 \times 10^{-5} \text{ gH}_2\text{O m}^{-3} (\text{mgCO}_2 \text{ m}^{-3})^{-1}$ (Table 1). Assuming the infrared analyzers for H₂O have the lowest sensitivity-to-CO₂ uncertainty for air flow with an atmospheric background CO₂ amount (i.e., 760 $\text{mgCO}_2 \text{ m}^{-3}$), $\Delta\rho_{CO_2}^s$ could be formulated as

$$350 \quad \Delta\rho_{H_2O}^s = s_{CO_2} (\rho_{CO_2} - 760) \quad \rho_{CO_2} \leq 1,553 \text{ mgCO}_2 \text{ m}^{-3}. \quad (20)$$

Accordingly, $\Delta\rho_{CO_2}^s$ can be reasonably expressed as

$$|\Delta\rho_{H_2O}^s| \leq 793 s_{CO_2}. \quad (21)$$

5.3 $\Delta\rho_{H_2O}$ (H₂O measurement accuracy)

Substituting Eqs. (16), (18), (19) and (21) into Model (15), $\Delta\rho_{H_2O}$ for an individual H₂O measurement from OPEC systems
 355 can be expressed as

$$\Delta\rho_{H_2O} = \pm \left[1.96\sigma_{H_2O} + 793 |s_{CO_2}| + \frac{|d_{wz}| + \delta_{H_2O_g}\rho_{H_2O}}{T_{rh} - T_{rl}} \times \begin{cases} T_a - T_c & T_c < T_a < T_{rh} \\ T_c - T_a & T_c > T_a > T_{rl} \end{cases} \right]. \quad (22)$$

This equation is the H₂O accuracy equation for the OPEC systems with infrared analyzers. It expresses the accuracy of H₂O measurements from the OPEC systems in terms of the specifications σ_{H_2O} , s_{CO_2} , d_{wz} , $\delta_{H_2O_g}$, T_{rh} , and T_{rl} ; measured variables



360 ρ_{H_2O} and T_a ; and a known variable T_c . Using this equation and the system specification values in Table 1, the accuracy of field H₂O measurements can be evaluated as a range.

5.4 Evaluation of $\Delta\rho_{H_2O}$

H₂O accuracy ($\Delta\rho_{H_2O}$) can be evaluated using the H₂O accuracy equation over a domain of T_a and ρ_{H_2O} . Similar to the CO₂ accuracy equation in Fig. 2, $\Delta\rho_{H_2O}$ is presented as the ordinate along the abscissa of T_a at different ρ_{H_2O} levels within the ranges of T_a and ρ_{H_2O} in ecosystems (Fig. 3). As with the evaluation of $\Delta\rho_{CO_2}$, T_a is limited from -30 to 50 °C and T_c can be
365 assumed to be 20 °C. The range of ρ_{H_2O} at T_a needs to be determined using atmospheric physics (Buck, 1981).

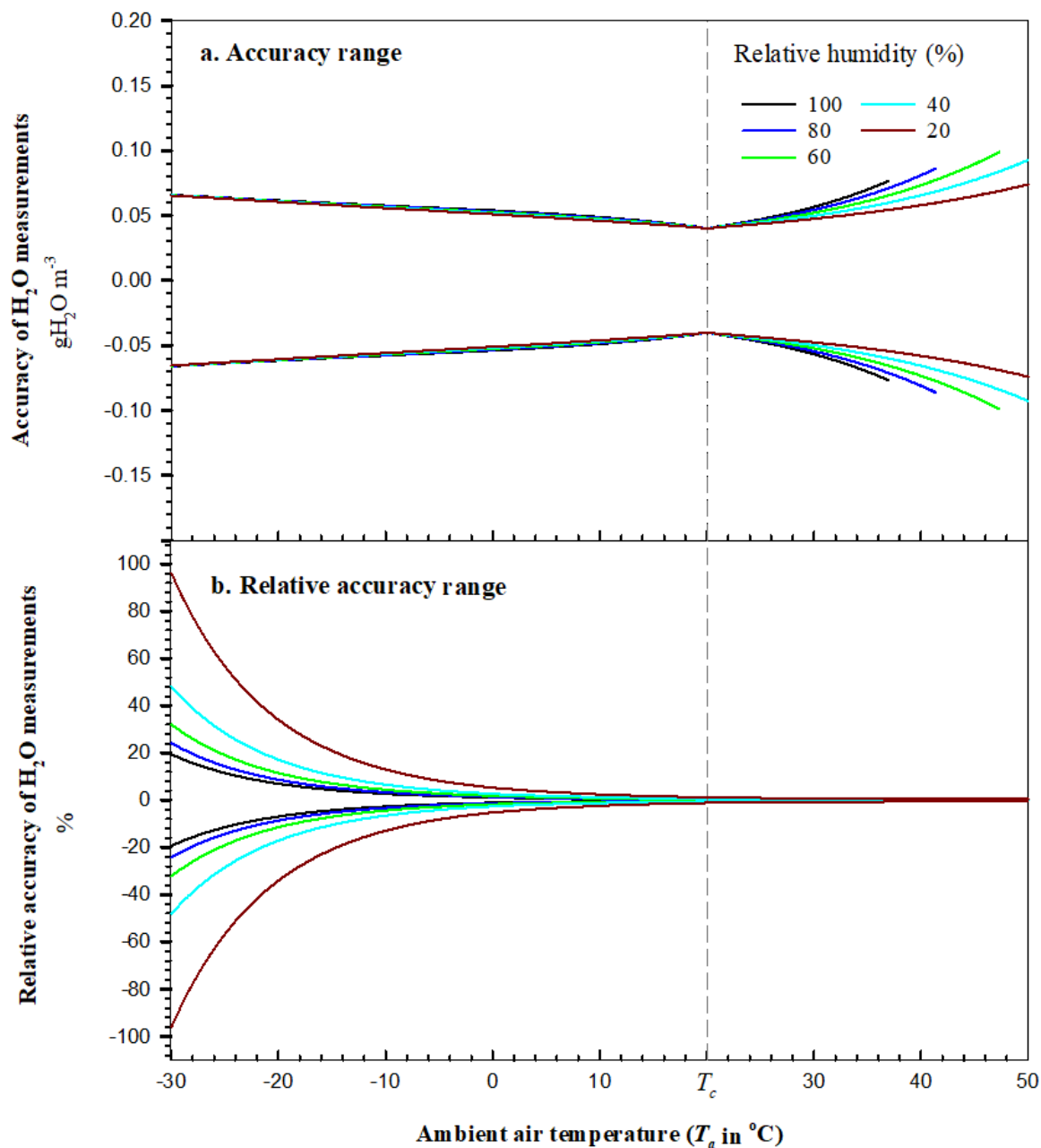
5.4.1 ρ_{H_2O} range

The analyzers measure H₂O density from 0 to 44 gH₂O m⁻³. However, due to the positive exponential dependence of air water vapor saturation on T_a (Wallace and Hobbs, 2006), ρ_{H_2O} has a range that is wider at higher T_a and narrower at lower T_a . Below 37 °C at 101.325 kPa, ρ_{H_2O} is lower than 44 gH₂O m⁻³, and its range becomes narrower and narrower, reaching 0.34
370 gH₂O m⁻³ at -30 °C. To determine the H₂O accuracy over the same relative range of air moisture, even at different T_a , the water vapor saturation density is used to scale air moisture to 20 , 40 , 60 , 80 and 100% (i.e., relative humidity, or RH). For each scaled RH value, ρ_{H_2O} can be calculated at different T_a and P (Appendix B) for use in the H₂O accuracy equation. In this way, over the range of T_a , H₂O accuracy can be shown as curves with equal RH (Fig. 3).

5.4.2 $\Delta\rho_{H_2O}$ range

375 In the same way as with CO₂ accuracy, the H₂O accuracy at $T_a = T_c$ is best at its narrowest as the sum of precision and sensitivity-to-CO₂ uncertainties (<0.040 gH₂O m⁻³ in magnitude). However, away from T_c , its non-linear range becomes wider, very gradually below this T_c value but more abruptly above, because, as T_a increases, ρ_{H_2O} at the same RH increases exponentially (Eqs. B1 and B2 in Appendix B) while $\Delta\rho_{H_2O}$ increases linearly with ρ_{H_2O} in the H₂O accuracy equation (22). This non-linear range can be summarized as the widest at 48 °C to be ± 0.099 gH₂O m⁻³ for air with 60% RH (Fig. 3a and
380 H₂O columns in Table 2). The number can be rounded up to ± 0.10 gH₂O m⁻³ for the overall accuracy of field H₂O measurements from OPEC systems by the EC150 infrared analyzers.

Fig. 3b shows an interesting trend of H₂O relative accuracy with T_a . Given the RH range shown in Fig. 3b, the relative accuracy diverges with a T_a decrease and converges with a T_a increase. The H₂O relative accuracy varies from 0.17% for saturated air at 37 °C to 96% for 20% RH air at -30 °C (data for Fig. 3b) and, at this low T_a , can be much greater if RH
385 goes further lower. The H₂O relative accuracy in magnitude is $< 1\%$ while $\rho_{H_2O} > 5.00$ gH₂O m⁻³, $< 5\%$ while $\rho_{H_2O} > 1.20$ gH₂O m⁻³, and $>10\%$ while $\rho_{H_2O} < 0.60$ gH₂O m⁻³.



390 **Figure 3.** Accuracy of field H_2O measurements from open-path eddy-covariance systems by EC150 infrared $\text{CO}_2\text{-H}_2\text{O}$ analyzers over their operational range in T_a under atmospheric pressure of 101.325 kPa. The vertical dashed line represents the ambient air temperature (T_c) at which an analyzer was calibrated, zeroed, and/or spanned. Relative accuracy of H_2O measurements is the ratio of H_2O accuracy to H_2O density.



6 Discussion

The primary objective of this study is to develop an assessment methodology to evaluate the overall accuracies of field CO₂ and H₂O measurements from OPEC systems by the infrared analyzers from their individual measurement uncertainties as specified using four uncertainty descriptors: zero drift, gain drift, sensitivity-to-CO₂/H₂O, and precision variability (Table 1). For the evaluation, these uncertainty descriptors are comprehensively composited into the accuracy model (2) formulated as a CO₂ accuracy equation (14) and an H₂O accuracy equation (22) (Sects. 3 to 5 and Appendix A). The assessment methodology, along with the model and the equations, is our development for the objective (Sects. 4.5 and 5.4). The evaluated accuracy can be used to assess CO₂ and H₂O data applications, and the formulated accuracy equations further provide rationales to assess and guide field maintenance on the infrared analyzers.

6.1 Methodology development

The methodology is developed from the derivation of accuracy model for the formulation of CO₂ and H₂O accuracy equations applicable in ecosystems to the evaluation of field CO₂ and H₂O measurement accuracies.

6.1.1 Accuracy model

Accuracy model (2) composites the four measurement uncertainties (zero drift, gain drift, sensitivity-to-CO₂/H₂O, and precision variability) specified for analyzer performance as an accuracy range. This range is modeled as a simple addition of the four uncertainties. The simple addition is derived from our analysis assertion that the four measurement uncertainties interactionally or independently contribute to the accuracy range, but the contribution from the interaction inside any pair of uncertainties is negligible because the interaction is three orders smaller in magnitude than an individual uncertainty in the pair (Appendix A). This derived model is simple and applicable, opening an approach to the formulation of accuracy equations that are computable to evaluate the overall accuracies of field CO₂ and H₂O measurements from OPEC systems by infrared analyzers.

6.1.2 Formulation of uncertainty terms in Model (2) for accuracy equations

In Sects. 4 and 5, each of the four uncertainty terms in accuracy model (2) is formulated as a computable sub-equation for CO₂ and H₂O, respectively (Eqs. 4, 7, 11, 13, 16, 18, 19, or 21). The accuracy model, whose terms are replaced with the formulated sub-equations for CO₂, becomes a CO₂ accuracy equation and, for H₂O, becomes an H₂O accuracy equation. In the formulation, approximation is used for zero drift, gain drift, and sensitivity-to-CO₂/H₂O, while statistics are applied for precision variability.

For the zero/gain drift, although it is well known that the drift is influenced more by T_a if housing CO₂-H₂O accumulation is assumed to be minimized as insignificant under normal field maintenance (LI-COR Biosciences, 2021b; Campbell Scientific Inc., 2021b), the exact relationship of drift to T_a does not exist. Alternatively, the zero/gain drift



uncertainty is formulated by an approximation of drifts away from T_c linearly in proportion to the difference between T_a and T_c but within its maximum range over the operational range in T_a of OPEC systems (Eqs. 7, 11, 18, and 19). A drift
425 uncertainty equation formulated through such an approximation is not an exact relationship of drift to T_a , but it does represent the drift trend, as influenced by T_a , to be understood by users. The accuracy from this equation at a given T_a is not exact either, but the maximum range over the full range, which is the most likelihood estimation, is most needed by users.

The sensitivity-to-CO₂/H₂O uncertainty can be formally formulated as Eq. (20) or (12), but, if directly used, this formulation would add an additional variable to the CO₂/H₂O accuracy equation. Equation (12) would add H₂O density
430 (ρ_{H_2O}) to the CO₂ accuracy equation, and Eq. (20) would add CO₂ density (ρ_{CO_2}) to the H₂O accuracy equation. For either accuracy equation, the additional variable would complicate the uncertainty analysis. According to the ecosystem environment background, the maximum range of sensitivity-to-CO₂/H₂O uncertainty is known and, compared to the zero/gain drift as a major uncertainty (Table 1), this range is narrow (Table 1 and Eqs. 13 and 21). Therefore, the sensitivity-to-CO₂/H₂O uncertainty is approximated as Eq. (21) or (13). This approximation widens the accuracy range slightly, in a
435 magnitude smaller than each of major uncertainties from the drifts at least in one order; however, it eliminates the need for ρ_{H_2O} in the CO₂ accuracy equation and for ρ_{CO_2} in the H₂O accuracy equation, which makes the equations easily applicable.

Precision uncertainty is statistically formulated as Eq. (4) for CO₂ and Eq. (16) for H₂O. This formulation is a common practice based on statistical methods (Hoel, 1984).

6.1.3 Use of relative accuracy for infrared analyzer specifications

440 Relative accuracy is often used concurrently with accuracy to specify sensor measurement performance. The accuracy is the numerator of relative accuracy whose denominator is the true value of a measured variable. When evaluated for the applications of OPEC systems in ecosystems, CO₂ accuracy magnitude is small in a range within one order (0.39 ~ 1.21 mgCO₂ m⁻³, data for Fig. 2a), and so is H₂O accuracy (0.04 ~ 0.10 gH₂O m⁻³, data for Fig. 3a). In ecosystems, CO₂ is naturally high, as compared to its accuracy magnitude, and does not change much in terms of a magnitude order (e.g., no
445 more than one order from 600 to 1,600 gH₂O m⁻³, assumed in this study). However, unlike CO₂, H₂O naturally changes in its amount dramatically across at least three orders in magnitude (e.g., at 101.325 kPa, from 0.03 gH₂O m⁻³ when RH is 10% at -30 °C to 40 gH₂O m⁻³ when dew point temperature is 35 °C at the highest as reported by National Weather Service (2021); under drier conditions, the H₂O amount could be even lower). Because, in ecosystems, CO₂ changes differently than H₂O in amount across magnitude orders, the relative accuracy behaviors in CO₂ differ from H₂O (Figs. 2b and 3b).

450 6.1.3.1 CO₂ relative accuracy

Because of the small CO₂ accuracy magnitude relative to the natural CO₂ amount in ecosystems, the CO₂ relative accuracy magnitude varies within a narrow range of 0.07 to 0.19% (Sect. 4.5.2). If the relative accuracy is used, either a range of 0.07 – 0.19% or an inequality of $\leq 0.19\%$ can be specified as the CO₂ relative accuracy magnitude for field CO₂ measurements.



Both range and inequality would be equivalently perceived by users to be a fair performance of OPEC systems. For
455 simplicity, our study with the OPEC systems can be specified for their CO₂ relative accuracy to be ±0.19%.

6.1.3.2 H₂O relative accuracy

Although the H₂O accuracy magnitude is also small, the “relatively” great change in natural air H₂O across several
magnitude orders in ecosystems results in a much wider range of the H₂O relative accuracy magnitude, from 0.23% at
460 maximum air moisture to 96% when RH is 20% at –30 °C (Fig. 3b and Sect. 5.4.2). H₂O relative accuracy can be much
greater under dry conditions at low T_a (e.g., 192% for air when RH is 10% at –30 °C). Accordingly, if the relative accuracy is
used, either a range of 0.23 – 192% or an inequality of $\leq 192\%$ can be specified as the H₂O relative accuracy magnitude for
field H₂O measurements. Either 0.23 – 192% or $\leq 192\%$ could be perceived by users intrinsically as poor measurement
performance of the infrared analyzers, although either specification is conditionally right for fair H₂O measurement.

Apparently, the relative accuracy for H₂O measurements in ecosystems is not intrinsically interpretable by users to
465 correctly perceive the performance of OPEC systems. Instead, if H₂O relative accuracy is unconditionally specified just in an
inequity of $\leq 192\%$, it could easily mislead users to wrongly assess the performance of OPEC systems as unacceptable for
H₂O measurements, although this performance of OPEC systems is fair for air when RH is 10% at –30 °C. Therefore, H₂O
relative accuracy is not recommended to be used for specification of infrared analyzers for H₂O measurement performance.
If this descriptor is used, the H₂O relative accuracy under a standard condition should be specified. This condition may be
470 defined as saturated air at 35 °C (i.e., the highest natural dew point (National Weather Service, 2021)) under normal P of
101.325 kPa (Wright et al., 2003). For our study case, under such a standard condition, the H₂O relative accuracy can be
specified within ±0.18% after manufacturing calibration (data for Fig. 3b).

6.2 Application of H₂O accuracy in data use

The measured variables ρ_{H_2O} , T_s and P can be used to compute T_a (Swiatek, 2018). If $T_a(\rho_{H_2O}, T_s, P)$ were an exact function
475 from the theoretical principles, it would not have any error itself. However, in our applications, variables ρ_{H_2O} , T_s , and P are
measured from the OPEC systems experiencing seasonal climates. As addressed in this study, the measured values of these
variables have measurement uncertainty in ρ_{H_2O} ($\Delta\rho_{H_2O}$, i.e., accuracy of field H₂O measurement); in T_s (ΔT_s , i.e., accuracy of
field T_s measurement); and in P (ΔP , i.e., accuracy of field P measurement). The uncertainties from measurement propagate
to the computed T_a as an uncertainty (ΔT_a , i.e., accuracy of $T_a(\rho_{H_2O}, T_s, P)$). This accuracy is a reference by any application
480 of T_a . It should be specified through its relationship of ΔT_a to $\Delta\rho_{H_2O}$, ΔT_s , and ΔP .

As field measurement uncertainties, $\Delta\rho_{H_2O}$, ΔT_s , or ΔP are reasonably small increments in numerical analysis
(Burden et al., 2016). As such, depending on all the small increments, ΔT_a is a total differential of $T_a(\rho_{H_2O}, T_s, P)$ with
respect to ρ_{H_2O} , T_s , and P , which are measured independently by three sensors, given by



$$\Delta T_a = \pm \left(\frac{\partial T_a}{\partial \rho_{H_2O}} \Delta \rho_{H_2O} + \frac{\partial T_a}{\partial T_s} \Delta T_s + \frac{\partial T_a}{\partial P} \Delta P \right). \quad (23)$$

485 In this equation, $\Delta \rho_{H_2O}$ from the application of Eq. (22) is a necessary term to acquire ΔT_a , ΔT_s can be acquired from the specifications for 3-D sonic anemometers (Zhou et al., 2018), ΔP can be acquired from the specifications for the barometer used in the OPEC systems (Vaisala, 2020), and the three partial derivatives can be derived from the explicit function $T_a(\rho_{H_2O}, T_s, P)$. With $\Delta \rho_{H_2O}$, ΔT_s , ΔP , and the three partial derivatives, ΔT_a can be ranged as a function of ρ_{H_2O} , T_s , and P .

6.3 Application of accuracy equations in analyzer field maintenance

490 An infrared analyzer performs better if the field environment is near its manufacturing conditions (e.g., T_a at 20 °C), which is demonstrated in Figs. 2a and 3a for measurement accuracies associated with T_c . As indicated by the accuracies in both figures, the closer to T_c at 20 °C while T_a is, the better analyzers perform. However, the analyzers are mostly used in OPEC systems for long-term field campaigns through four-seasonal climates vastly different from those in the manufacturing processes. Over time, an analyzer gradually drifts in some ways and needs field maintenance although within its
495 specifications.

The field maintenance cannot improve the sensitivity-to-CO₂/H₂O uncertainty and precision variability, but both are minor (their sum < 0.392 mgCO₂ m⁻³ for CO₂, Eqs. 4 and 13; < 0.045 gH₂O m⁻³ for H₂O, Eqs. 16 and 21) as compared to the zero or gain drift uncertainties. However, the zero and gain drift uncertainties are major in determination of field CO₂/H₂O measurement accuracy (Figs. 2 to 4 and Eqs. 14 and 22), but adjustable, through the zero and/or span procedures, to be
500 minimized. Therefore, manufacturers of infrared analyzers have provided software and hardware tools for the procedures (Campbell Scientific Inc., 2021b) and scheduled the procedures using those tools (LI-COR Biosciences, 2021b). This study provides rationales how to assess, schedule, and perform the procedures (Figs. 2a, 3a, and 4).

6.3.1 CO₂ zero and span procedures

Figure 4a shows that the CO₂ zero drift uncertainty linearly increases with T_a away from T_c over the full T_a range within
505 which OPEC systems operate; so, too, does CO₂ gain drift uncertainty increase for a given CO₂ concentration. As suggested by Zhou et al. (2021), both drifts should be adjusted near the T_a value around which the system runs. The zero and gain drifts should be adjusted, through zero and span procedures, at a T_a close to its daily mean around which the system runs. Based on the range of T_a daily cycle, the procedures are set at a moderate, instead of the highest or lowest, moment in T_a . Given the daily cycle range is much narrower than 40 °C, an OPEC system could run at T_a within ±20 of T_c if the procedures are
510 performed at a right moment of T_a . For our study case on atmospheric CO₂ background (left CO₂ column in Table 2), the procedures can narrow the widest possible range of ±1.21 mgCO₂ m⁻³ for field CO₂ measurement at least 40% to ±0.72 mgCO₂ m⁻³ (i.e., accuracy at 0 or 40 °C when $T_c = 20$ °C), which would be a significant improvement to ensure field CO₂ measurement accuracy through CO₂ zero and span procedures.



6.3.2 H₂O zero and span procedures

515 Figure 4b shows that the H₂O zero drift uncertainty increases as T_a moves away from T_c in the same trend as CO₂ zero drift
uncertainty. Therefore, an H₂O zero procedure can be performed in the same technique as for CO₂ zero procedure. H₂O gain
drift uncertainty has a different trend. It exponentially diverges, as T_a increases away from T_c , to $\pm 5.0 \times 10^{-2}$ gH₂O m⁻³ near
50 °C, and gradually converges by two orders smaller, as T_a decreases away from T_c , to $\pm 6.38 \times 10^{-4}$ gH₂O m⁻³ at -30 °C
(data for Fig. 4b). The exponential divergence results from the linear relationship of H₂O gain drift uncertainty (Eq. 19) with
520 ρ_{H_2O} , which exponentially increases (Eq. B1) with a T_a increase away from T_c for the same RH (Buck, 1981). The
convergence results from the linear relationship offset by the exponential decrease in ρ_{H_2O} with a T_a decrease for the same
RH. This trend of H₂O gain drift uncertainty with T_a is a rationale to guide the H₂O span procedure, which adjusts the H₂O
gain drift.

The H₂O span procedure needs standard moist air with known H₂O density from a dew point generator. The
525 generator is not operational near or below freezing conditions (LI-COR Biosciences, 2004), which limits the span procedure
to be performed only under non-freezing conditions. This condition, from 5 to 35 °C, may be considered for the generator to
be conveniently operational in the field. Accordingly, the H₂O zero and span procedures should be discussed separately for a
 T_a above and below 5 °C.

6.3.2.1 T_a above 5 °C

530 Looking at the right portion with T_a above 5 °C in Fig. 4b, H₂O gain drift has a more obvious impact on measurement
uncertainty in a higher T_a range (e.g., above T_c), within which the H₂O span procedure is most needed. In this range, the
maximum accuracy range of ± 0.10 gH₂O m⁻³ can be narrowed by 30% to ± 0.07 (assessed from data for Fig 3a) if H₂O zero
and span procedures can be sequentially performed as necessary in a T_a range from 5 to 35 °C.

6.3.2.2 T_a below 5 °C

535 Looking at the left portion with T_a below 5 °C in Fig 4b, H₂O gain drift has a less obvious contribution to the measurement
uncertainty in a lower T_a range (e.g., below 5 °C), within which the H₂O span procedure may be unnecessary. An H₂O gain
drift uncertainty at 5 °C is 50% of the H₂O zero drift uncertainty (dotted curve in Fig. 5). This percentage decreases to 3% at
-30 °C. On average, this percentage over a range of -30 to 5 °C is 18% (assessed from data for dotted curve in Fig. 5). Thus,
for H₂O measurements over the lower T_a range, it can be concluded that H₂O zero drift is a major uncertainty source, and
540 H₂O gain drift is a minor uncertainty source.

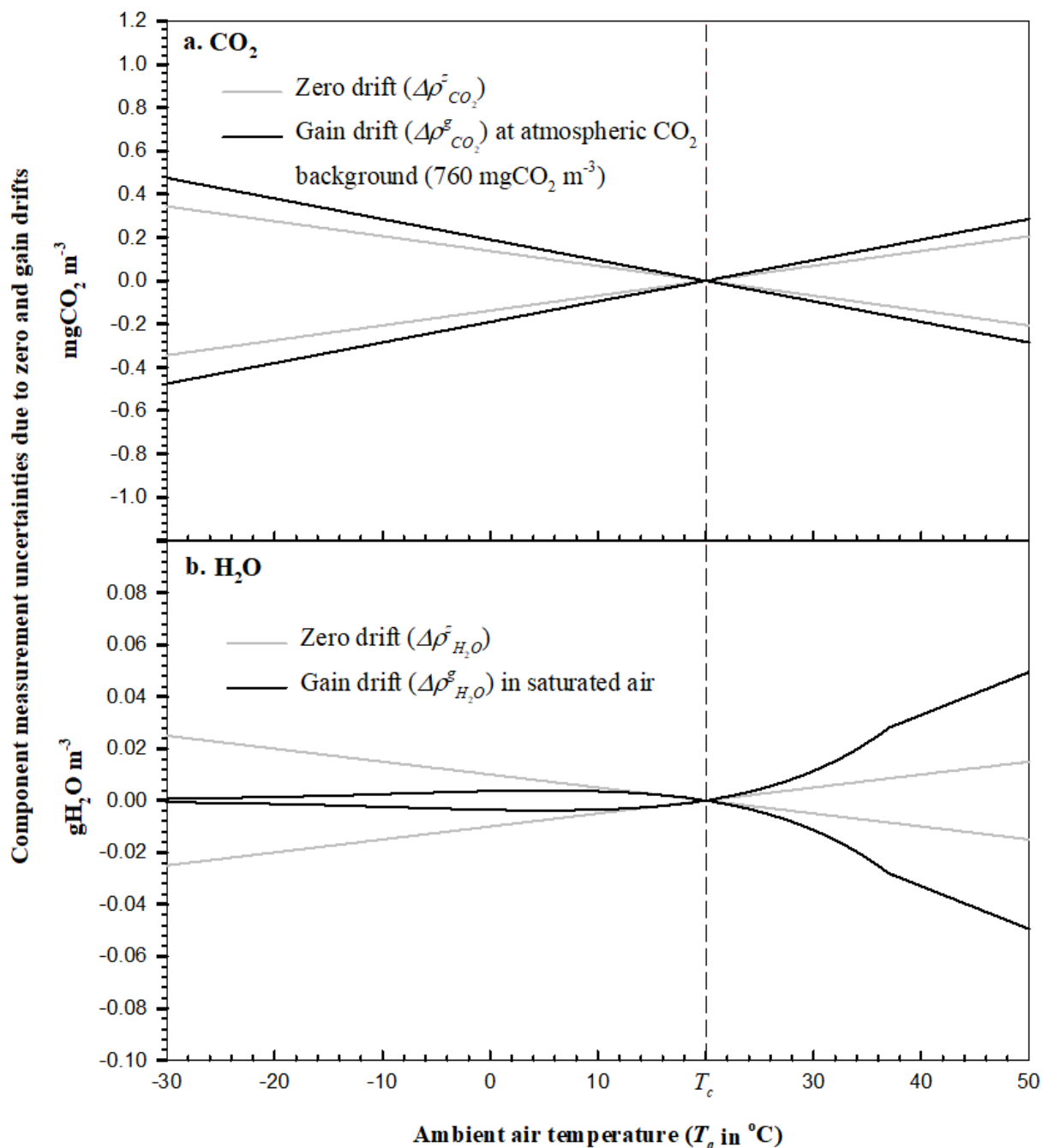
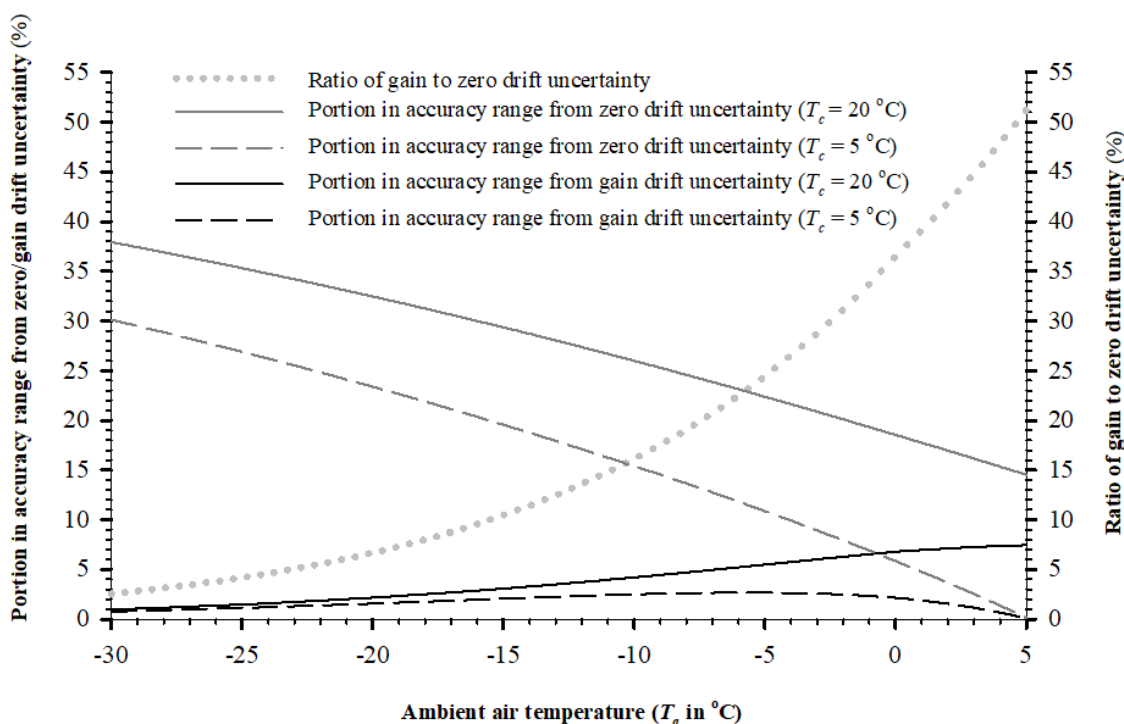


Figure 4. Component measurement uncertainties due to the zero and gain drifts of EC150 infrared CO₂–H₂O analyzers in open-path eddy-covariance flux systems over their operational range in T_a under an atmospheric pressure of 101.325 kPa. The vertical dashed line represents the ambient temperature (T_c) at which an analyzer was calibrated, zeroed, and/or spanned.



545 A close examination of the other curves in Fig. 5 for the portion in the accuracy range from H₂O zero/gain drift
makes this conclusion more convincing. Given $T_c = 20$, in accuracy range, the portion from H₂O zero drift uncertainty is
much greater (maximum 38% at -30 °C) than that from H₂O gain drift uncertainty (maximum only 7% at 5 °C). On average
over the lower T_a range, the former is 27% and the latter only 4%. Further, given $T_c = 5$ °C, in the accuracy range, the portion
550 from H₂O gain drift uncertainty is even smaller (maximum only 3% at -5 °C); in contrast, the portion from zero drift
uncertainty is more major (one order higher, 30% at -30 °C). On average over the lower T_a range, the minor gain drift
uncertainty is 1.7%, and the major zero drift uncertainty is 17%. Both percentages underscore that the H₂O span procedure is
reasonably unnecessary under cold/dry conditions, and, under such conditions, the H₂O zero procedure is the only necessary
option to efficiently minimize H₂O measurement uncertainty in OPEC systems. This finding gives confidence in H₂O
measurement accuracy to users who are worried about H₂O span procedures for infrared analyzers in the cold seasons when
555 a dew point generator is not operational in the field (LI-COR Biosciences, 2004).



560 **Figure 5.** For a range of low T_a , the portion in the accuracy range from zero/gain drift uncertainty (left ordinate) and the ratio
of gain to zero drift uncertainty (right ordinate). The curves are evaluated by Eqs. (18), (19), and (22) from measurement
specifications for EC150 infrared CO₂–H₂O analyzers in open-path eddy-covariance flux systems over the T_a range from -30
to 5 °C under atmospheric pressure of 101.325 kPa. T_c is the ambient air temperature at which an analyzer was calibrated,
zeroed, and/or spanned.



6.3.3 H₂O zero procedure in cold and/or dry environments

In cold environments, although the non-operational H₂O span procedure is unnecessary, the H₂O zero procedure is asserted to be a prominently important option for minimizing the H₂O measurement uncertainty in OPEC systems. This procedure, although operational under freezing conditions, is still inconvenient for users when weather is very cold (e.g., when T_a is below $-15\text{ }^\circ\text{C}$). If the field H₂O zero procedure is performed as needed above this T_a value, an OPEC system can be assumed to run at T_a with $\pm 20\text{ }^\circ\text{C}$ of T_c . Under this assumption, the poorest H₂O accuracy of $\pm 0.066\text{ gH}_2\text{O m}^{-3}$ below $5\text{ }^\circ\text{C}$ in Table 2 can be narrowed, through the H₂O zero procedure, by at least 22% to $0.051\text{ gH}_2\text{O m}^{-3}$ (assessed from data for Fig. 3a). Correspondingly, the relative accuracy range can be narrowed by the same percentage. The H₂O zero procedure can ensure both accuracy and relative accuracy of H₂O measurements in a cold environment. In a dry environment, it plays the same role as in a cold environment, but it would be more convenient for users if warmer.

In a cold and/or dry environment, H₂O zero procedures that are undergone on a regular schedule would best minimize the impact of zero drifts on measurements. Under such an environment, the automatic zero procedure for CO₂ and H₂O together in CPEC systems is an operational and efficient option to ensure and improve field CO₂ and H₂O measurement accuracies (Campbell Scientific Inc., 2021a; Zhou et al., 2021).

7 Conclusions

The accuracy of field CO₂/H₂O measurements from OPEC systems by the infrared analyzers can be defined as a maximum range of composite measurement uncertainty sourced from component uncertainties: zero drift, gain drift, sensitivity-to-CO₂/H₂O, and precision variability, all of which are included in the system specifications (Table 1). The specified uncertainties interactionally or independently contribute to the overall uncertainty. Fortunately, the interactions between component uncertainties in each pair is three orders smaller than either component individually (Appendix A). Therefore, these specified uncertainties can be simply added as the accuracy range in a general CO₂/H₂O accuracy model for OPEC systems (Model 2). Based on statistics, bio-environment, and approximation, the specification descriptors of the infrared analyzers in OPEC systems are incorporated into the model terms to formulate the CO₂ accuracy equation (14) and the H₂O accuracy equation (22), both of which are computable to evaluate corresponding CO₂ and H₂O accuracies. For the OPEC systems in this study over their operational range in T_a at the standard P of 101.325 kPa (Figs. 2 and 3 and Table 2), the CO₂ accuracy can be specified as $\pm 1.21\text{ mgCO}_2\text{ m}^{-3}$ (relatively within $\pm 0.19\%$, Fig. 2) and H₂O accuracy as $\pm 0.10\text{ gH}_2\text{O m}^{-3}$ (relatively within $\pm 0.18\%$ for saturated air at $35\text{ }^\circ\text{C}$ at the standard P , Fig. 3).

Both accuracy equations are not only applicable for further error/uncertainty analyses in CO₂ and H₂O data applications (see Sect. 6.1), but they also may be used as a rationale to assess and guide field maintenance on infrared analyzers. Combining Eq. (14) as shown in Fig. 2a with Eqs. (7) and (11) as shown in Fig. 4a guides users to adjust the CO₂ zero and gain drifts, through the corresponding zero and span procedures, near the middle of the T_a range within which the analyzer runs. As assessed on atmospheric background, the procedures can narrow the maximum CO₂ accuracy range by



595 40%, from ± 1.21 to ± 0.72 $\text{mgCO}_2 \text{ m}^{-3}$, and thereby greatly improve the CO_2 measurement accuracies with these regular CO_2 zero and span procedures.

Equation (22) as shown in Fig. 3a, plus Eqs. (18) and (19) as shown in Fig. 4b, present users with a rationale to adjust the H_2O zero drift of analyzers in the same technique as for CO_2 , but the H_2O gain drift under hot and humid environments needs more attention (see the right portion above T_c in Figs. 3a and 4b); under cold and/or dry environments, it needs no further concern (see the left portion below 0°C in Fig. 4b). In a T_a range above 5°C , the maximum H_2O accuracy range of ± 0.10 $\text{gH}_2\text{O m}^{-3}$ can be narrowed by 30% to ± 0.07 $\text{gH}_2\text{O m}^{-3}$ if both H_2O zero and span procedures are performed as necessary. In a T_a range below 5°C , the H_2O zero procedure alone can narrow the maximum H_2O accuracy range of ± 0.076 $\text{gH}_2\text{O m}^{-3}$ by 22%, to ± 0.051 $\text{gH}_2\text{O m}^{-3}$. Under cold environmental conditions, the H_2O span procedure is found to be unnecessary (Fig. 5), and the H_2O zero procedure is proposed as the only, and prominently efficient, option to minimize H_2O measurement uncertainty in OPEC systems. This procedure plays the same role under dry conditions. Under cold and/or dry environments, the zero procedure for CO_2 and H_2O together would be a practical and efficient option to not only warrant, but also to improve, measurement accuracy. In a cold environment, adjusting the H_2O gain drift is impractical because of a dew point generator that fails to generate standard H_2O gas near freezing conditions. This lack of necessity relieves user worry with regard to H_2O measurement uncertainty from the H_2O gain drift under such environments where the H_2O span procedure is not operational.

Additionally, as a specification descriptor for OPEC systems used in ecosystems, relative accuracy is applicable for CO_2 instead of H_2O measurements because, in ecosystems, the CO_2 relative accuracy varies slightly within a magnitude order, and the H_2O relative accuracy varies dramatically across several magnitude orders. A small range in the CO_2 relative accuracy can be perceived intuitively by users as normal. In contrast, without specifying the condition of air moisture, a large range in H_2O relative accuracy under cold and/or dry conditions (e.g., 100%) can easily mislead users to automatically transfer this relative accuracy onto very poor H_2O measurements, although, under such conditions, it is the best that modern technology can do in the field. The authors suggest to conditionally define H_2O relative accuracy at 35°C dew point (i.e., 39.66 $\text{gH}_2\text{O m}^{-3}$ at 101.352 kPa). Ultimately, this study provides our logic to the flux community in specifying the accuracy of CO_2 – H_2O measurement from OPEC systems by infrared analyzers.

620 **Appendix A: Derivation of accuracy model for infrared CO_2 – H_2O analyzers**

As defined in the Introduction, the measurement accuracy of infrared CO_2 – H_2O analyzers is a range of the difference between the true α density ($\rho_{\alpha T}$, where α can be either H_2O or CO_2) and measured α density (ρ_a) by the analyzer. The difference is denoted by $\Delta\rho_a$, given by Eq. (1) in Sect. 3. Analyzer performance uncertainties contribute to this range, as specified in the four descriptors: zero drift, gain drift, cross-sensitivity, and precision (LI–COR Biosciences, 2021b; Campbell Scientific Inc., 2021b).



According to the definitions in Sect. 2, zero drift uncertainty ($\Delta\rho_{\alpha}^z$) is independent of $\rho_{\alpha T}$ value and gain trend related to analyzer response; so, too, is cross-sensitivity uncertainty ($\Delta\rho_{\alpha}^s$), which depends upon the amount of background H₂O in the measured air if α is CO₂, and upon the amount of background CO₂ in the measured air if α is H₂O. In the case that both gain drift and precision uncertainties are zero, $\Delta\rho_{\alpha}^z$ and $\Delta\rho_{\alpha}^s$ are simply additive to any true value as a measured value, including zero drift and cross-sensitivity uncertainties ($\rho_{\alpha_{zs}}$)

$$\rho_{\alpha_{zs}} = \rho_{\alpha T} + \Delta\rho_{\alpha}^z + \Delta\rho_{\alpha}^s, \quad (\text{A1})$$

where subscript z indicates zero drift uncertainty included in the measured value, and subscript s indicates cross-sensitivity uncertainty included in the measured value. During the measurement process, while zero is drifting and cross-sensitivity is active, if gain also drifts, then the gain drift interacts with the zero drift and the cross-sensitivity. This is because $\rho_{\alpha_{zs}}$ is a linear factor for this gain drift (see the cells in gain-drift row and value columns in Table 1) that is added to $\rho_{\alpha_{zs}}$ as a measured value additionally including gain drift uncertainty ($\rho_{\alpha_{zsg}}$, where subscript g indicates gain drift uncertainty included in the measured value), given by

$$\rho_{\alpha_{zsg}} = \rho_{\alpha_{zs}} + \delta_{\alpha_g} \rho_{\alpha_{zs}}, \quad (\text{A2})$$

where δ_{α_g} is gain drift percentage ($\delta_{CO_2_g} = 0.10\%$ and $\delta_{H_2O_g} = 0.30\%$, Table 1). Substituting $\rho_{\alpha_{zs}}$ in this equation with Eq. (A1) leads to

$$\rho_{\alpha_{zsg}} = \rho_{\alpha T} + \Delta\rho_{\alpha}^z + \Delta\rho_{\alpha}^s + \delta_{\alpha_g} \rho_{\alpha T} + \delta_{\alpha_g} \Delta\rho_{\alpha}^z + \delta_{\alpha_g} \Delta\rho_{\alpha}^s. \quad (\text{A3})$$

In this equation, $\delta_{\alpha_g} \Delta\rho_{\alpha}^z$ is the zero-gain interaction, and $\delta_{\alpha_g} \Delta\rho_{\alpha}^s$ is the sensitivity-gain interaction. In magnitude, the former is three orders smaller than either zero drift uncertainty ($\Delta\rho_{\alpha}^z$) or gain drift uncertainty ($\delta_{\alpha_g} \rho_{\alpha T}$). The sensitivity-gain interaction is three orders smaller than either cross-sensitivity uncertainty ($\Delta\rho_{\alpha}^s$) or gain drift uncertainty. Therefore, both interactions are relatively small and can be reasonably dropped. As a result, Eq. (A3) can be approximated and rearranged as:

$$\begin{aligned} \rho_{\alpha_{zsg}} &\approx \rho_{\alpha T} + \Delta\rho_{\alpha}^z + \delta_{\alpha_g} \rho_{\alpha T} + \Delta\rho_{\alpha}^s \\ &= \rho_{\alpha T} + \Delta\rho_{\alpha}^z + \Delta\rho_{\alpha}^g + \Delta\rho_{\alpha}^s, \end{aligned} \quad (\text{A4})$$

where $\Delta\rho_{\alpha}^g$ is gain drift uncertainty. Any measured value has random error (i.e., precision uncertainty) independent of $\rho_{\alpha T}$ in value (ISO, 2012). Therefore, $\rho_{\alpha_{zsg}}$ plus precision uncertainty ($\Delta\rho_{\alpha}^p$) is the measured value including all uncertainties (ρ_{α}), given by

$$\rho_{\alpha} = \rho_{\alpha_{zsg}} + \Delta\rho_{\alpha}^p. \quad (\text{A5})$$

The insertion of Eq. (A4) into this equation leads to

$$\rho_{\alpha} - \rho_{\alpha T} = \Delta\rho_{\alpha}^z + \Delta\rho_{\alpha}^g + \Delta\rho_{\alpha}^s + \Delta\rho_{\alpha}^p. \quad (\text{A6})$$



This equation holds

$$\Delta\rho_a \leq |\Delta\rho_a^z| + |\Delta\rho_a^g| + |\Delta\rho_a^s| + |\Delta\rho_a^p|. \quad (\text{A7})$$

655 The range of the right side of this equation is wider than the measurement uncertainty from all measurement uncertainty sources and the difference of ρ_a minus ρ_{aT} (i.e., $\Delta\rho_a$). Using this range, the measurement accuracy is defined in Model (2) in Sect. 3.

Appendix B: Water vapor density from ambient air temperature, relative humidity, and atmospheric pressure

660 Given ambient air temperature (T_a in °C) and atmospheric pressure (P in kPa), air has a limited capacity to hold an amount of water vapor (Wallace and Hobbs, 2006). This limited capacity is described in terms of saturation water vapor density (ρ_s in $\text{gH}_2\text{O m}^{-3}$) for moist air, given through the Clausius–Clapeyron equation (Sonntag, 1990; Wallace and Hobbs, 2006)

$$\rho_s(T_a, P) = \frac{0.6112f(P)}{R_v(273.15 + T_a)} \begin{cases} \exp\left(\frac{17.62T_a}{T_a + 243.12}\right) & T_a \geq 0 \\ \exp\left(\frac{22.46T_a}{T_a + 272.62}\right) & T_a < 0 \end{cases}, \quad (\text{B1})$$

665 where R_v is the gas constant for water vapor ($4.61495 \times 10^{-4} \text{ kPa m}^3 \text{ K}^{-1} \text{ gH}_2\text{O}^{-1}$), and $f(P)$ is an enhancement factor for moist air, being a function of P : $f(P) = 1.0016 + 3.15 \times 10^{-5} P - 0.0074 P^{-1}$. At relative humidity (RH in %), the water vapor density [$\rho_{\text{H}_2\text{O}}^{\text{RH}}(T_a, P)$ in $\text{gH}_2\text{O m}^{-3}$] is

$$\rho_{\text{H}_2\text{O}}^{\text{RH}}(T_a, P) = \text{RH}\rho_s(T_a, P). \quad (\text{B2})$$

This equation, along with Eq. (B1), is used to calculate $\rho_{\text{H}_2\text{O}}^{\text{RH}}$ used in Fig. 3 in Sect. 5 and Figs. 4b and 5 in Sect. 6.3.

Acknowledgements. Authors thank Brittney Smart for her dedicated revision and Linda Worlton-Jones for her professional proofreading.

670 *Financial support.* This research has been supported by the Strategic Priority Research Program of the Chinese Academy of Sciences (grant no. XDA19030204), Campbell Scientific Research and Development, Campbell Scientific Inc. (project no. 14433), National Key Research and Development Program of China (grant no. 2016YFD0600206), and Long-Term Agroecosystem Research, USDA (award no. 58-3042-9-014).



References

- Aubinet, M., Vesala, T., and Papale, D. (eds): Eddy Covariance: A Practice Guide to Measurement and Data Analysis, Springer, New York, 438 p, <https://doi.org/10.1007/978-94-007-2351-1>, 2012.
- Buck, A. L.: New equations for computing vapor pressure and enhancement factor, *Journal of Applied Meteorology*, 20: 1527–1532, [https://doi.org/10.1175/1520-0450\(1981\)020<1527:NEFCVP>2.0.CO;2](https://doi.org/10.1175/1520-0450(1981)020<1527:NEFCVP>2.0.CO;2), 1981.
- Burden, R. L., Faires, J. D., and Burden, A.M: Numerical Analysis, 10th ed., Gengage Learning, Boston, 896 p., 2016.
- Campbell Scientific Inc.: CPEC300/306/310 CO₂/H₂O Closed-Path Eddy-Covariance Systems, Revision 08/21, Logan, UT, USA, 92 p., 2021a.
- Campbell Scientific Inc.: EC150 CO₂/H₂O Open-Path Gas Analyzer, Revision 09/21, Logan, UT, USA, 41 p., 2021b.
- 685 Csavina, J., Roberti, J. A., Taylor, J. R., and Loescher, H. W.: Traceable measurements and calibration: A primer on uncertainty analysis, *Ecosphere*, 8(2): e01683, <http://doi.wiley.com/10.1002/ecs2.1683>, 2017.
- Foken, T., Leuning, R., Onley, S. R., Mauder, M., Aubinet, M.: Correction and data quality control, In: Eddy Covariance: A Practice Guide to Measurement and Data Analysis, edited by Aubinet, M., Vesala, T., and Papale D., 85–131, Springer, New York, https://doi.org/10.1007/978-94-007-2351-1_4, 2012.
- 690 Global Monitoring Laboratory: Trends in Atmospheric Carbon Dioxide. Accessed October 01, 2021, <https://www.esrl.noaa.gov/gmd/ccgg/trends/weekly.html>, 2021.
- Hill, T., Chocholek, M., and Clement, R.: The case for increasing the statistical power of eddy covariance ecosystem study, where and how, *Global Change Biology*, 23: 2154–2165, <https://doi.org/10.1111/gcb.13547>, 2017.
- Hoel, P. G.: Introduction to Mathematical Statistics, 5th ed, John Wiley & Son, New York, 435 pp, 1984.
- 695 ISO: Accuracy (trueness and precision) of measurement methods and results — Part 1: General principles and definitions, ISO 5725-1, 1994 (reviewed in 2012), International Organization for Standardization, Geneva, Switzerland, 17 pp., 2012.
- Joint Committee for Guides in Metrology: Evaluation of measurement data: Guide to the expression of uncertainty in measurement, 1st ed, Research Triangle Park, NC, USA: JCGM Member Organization, 2008.
- 700 Lee, X. and Massman, W. J.: A Perspective on thirty years of the Webb, Pearman and Leuning density corrections, *Boundary-Layer Meteorology*, 139: 37–59, <https://doi.org/10.1007/s10546-010-9575-z>, 2011.
- LI-COR Biosciences: LI-610 Portable Dew Point Generator: Instruction Manual, 3-1~20, Lincoln, NE, USA, 2004.
- LI-COR Biosciences: LI-7200RS Closed CO₂/H₂O Gas Analyzer: Instruction Manual, p. 1-1~H-4, Lincoln, NE, USA, 2021a.
- 705 LI-COR Biosciences: Using the LI-7500DS Open Path CO₂/H₂O Gas Analyzer and the SmartFlux 3 Systems: Instruction Manual, 4-1~11 and 8-1~9, Lincoln, NE, USA, 2021b.
- McDermitt, D. K., Welles, J. M., and Eckles, R. D.: Effects of temperature, pressure and water vapor on gas phase infrared absorption by CO₂, LI-COR Application Note #116, 5 p., 1993.



- National Weather Service: Fast Facts, National Oceanic and Atmospheric Administration, Accessed October 01, 2021,
710 <https://www.weather.gov>, 2021.
- Ohkubo, S., Kosugi, Y., Takahashi, S., Matsuo, N., Tani, M., and Nik, A. R.: Vertical profiles and storage fluxes of CO₂,
heat and water in a tropical rainforest at Pasoh, Peninsular Malaysia, *Tellus*, 60B: 569–582,
<https://doi.org/10.1111/j.1600-0889.2008.00367.x>, 2018.
- Sonntag, D.: Important new values of the physical constants of 1986, vapor pressure formulation based on the ITC-90, and
715 psychrometer formulae, *Zeitschrift für Meteorologie*, 40: 340–344, 1990.
- Swiatek, E.: Derivation of Temperature (T_c) from the Sonic Virtual Temperature (T_s), Vapor Density (ρ_v)/Vapor Pressure (e)
and Pressure (P), Campbell Scientific Inc., Logan, UT, USA, 1–5 pp., 2018.
- Vaisala: Vaisala BAROCAP® Barometer PTB100 Series (User’s Guide), M210839EN-A, 1–4. Helsinki, Finland, 2020.
- Wallace, J. M. and Hobbs, P. V.: *Atmospheric Science: An Introductory Survey*, 2nd ed., Academic Press, Amsterdam, 350
720 pp., 2006.
- Wang, X., Wang, C., Guo, Q., and Wang, J.: Improving the CO₂ storage measurements with a single profile system in a tall-
dense-canopy temperate forest, *Agricultural and Forest Meteorology*, 228–229: 327–338,
<https://doi.org/10.1016/j.agrformet.2006.07.020>, 2016.
- Wright, J. D., Johnson, A. N., and Moldover, M. R.: Design and Uncertainty for a PVTt Gas Flow Standard, *Journal of*
725 *Research of the National Institute of Standards and Technology*, 108(1): 21–47, <https://doi.org/10.6028/jres.108.00>,
2003.
- Yang, B., Hanson, P. J., Riggs, J. S., Pallardy, S. G., Heuer, M. H., Hosman, K. P., Meyers, T. P., Wullschleger, S. D., Gu,
L. H.: Biases of CO₂ storage in eddy flux measurements in a forest pertinent to vertical configurations of a profile
system and CO₂ density averaging, *Journal of Geophysical Research*, 112: D20123,
730 <https://doi.org/10.1029/2006JD008243>, 2002.
- Zhou, X., Gao, T., Pang, Y., Manhan, H., Li, X., Zheng, N., Suyker, A. E., Awada, T., and Zhu., J.: Based on atmospheric
physics and ecological principle to assess the accuracies of field CO₂/H₂O measurements from infrared gas analyzers in
closed-path eddy-covariance systems, *Earth and Space Science*, 8, e2021EA001763,
<https://doi.org/10.1029/2021EA001763>, 2021.
- 735 Zhou, X., Yang, Q., Zhen, X., Li, Y., Hao, G., Shen., H., Gao, T., Sun, Y., Zheng, N.: Recovery of the 3-dimensional wind
and sonic temperature data from a physically deformed sonic anemometer, *Atmospheric Measurement Techniques*, 11:
5981–6002, <https://doi.org/10.5194/amt-11-5981-2018>, 2018.